NAME [redacted]

DATE 12/09/14

UNIVERSITY OF OKLAHOMA

GRADUATE COLLEGE

INTEGRATED CHARACTERIZATION OF THE WOODFORD SHALE IN THE SOUTHERN CHEROKEE PLATFORM, OKLAHOMA

A THESIS

SUBMITTED TO THE GRADUATE FACULTY

in partial fulfillment of the requirements for the

Degree of

MASTER OF SCIENCE

By

LUIS FELIPE CARDONA-VALENCIA
Norman, Oklahoma
2014

INTEGRATED CHARACTERIZATION OF THE WOODFORD SHALE IN THE SOUTHERN CHEROKEE PLATFORM, OKLAHOMA

A THESIS APPROVED FOR THE
CONOCOPHILLIPS SCHOOL OF GEOLOGY AND GEOPHYSICS

BY

[redacted]

Dr. Roger M. Slatt, Chair

[redacted]

Dr. Kurt J. Marfurt

[redacted]

Dr. R. Paul Philp

ACKNOWLEDGEMENTS

This manuscript is the end result of several months of analyses and interpretations which could not be possible without the dedicated and unconditional coaching, financial and technical support of my profoundly respected advisor Dr Roger Slatt. I am very grateful with life and him for allowing me to be part of the last cohort of students that he mentors. Life passes by in a flicker and I wish him all the best possible blessings in his personal and professional endeavors in the upcoming decades. I hope we can cross paths again sooner!

To my committee, Dr. Kurt Marfurt and Dr. Paul Philp, for their dedication to guide me through this educational and inspirational journey and for their time dedicated to review these lines. I am very much honored to have had them as technical reviewers.

Thanks to Dr Shankar Mitra and Dr Matthew Pranter for their coaching and friendship that have expanded my professional horizons.

This research would not be possible without the support of Pathfinder Exploration LLC, in particular Jerry Wilson, Luis Castillo and David Galvis whose ideas and wisdom greatly helped me to improve my knowledge. My gratitude also to AASPI consortium, CGG, and Schlumberger for providing the petrotechnical software that allowed processing the subsurface data for this research.

Special acknowledgements to the University of Oklahoma and the ConocoPhillips School of Geology and Geophysics for providing all infrastructure and staff resources that made me feel at home. Dr Douglas Elmore, Teresa Hackney, Devon Harr, Nancy Leonard, Jocelyn Cook, Rebecca Fay, and Donna Mullins: I will have you all in my hearth.

To my friends Lily Pfeifer, Pierre Karam, Roger Leavitt, Bryan Turner, Brenton McCullough, Jie Qie, Sumit Verma, David Lubo, Javier Tellez and Carolina Mayorga for being supportive and special.

To my wife Alejandra for her love, motivation and support along the road and through our years together. To my family for being close to my hearth despite the distance.

To God who walks by my side and whose presence guides my life and fills it with joy.

TABLE OF CONTENTS

LIST OF TABLES

LIST OF FIGURES

ABSTRACT

The Late Devonian-Early Mississippian, organic-rich Woodford Shale is considered as one of the most important unconventional resources for oil and gas in the United States of America. This formation was targeted for gas exploitation until 2008 mostly in the Anadarko and Arkoma basins (Oklahoma), however, recent studies in the Cherokee Platform of Oklahoma have demonstrated that there are large volumes of hydrocarbons at depths of 3,500 to 6,500 feet in Cleveland, Pottawatomie, and McClain Counties (Althoff, 2012).

This study characterizes the Woodford Shale in an area located in the southern end of the Cherokee Platform in order to identify its hydrocarbon reservoir potential by analyzing well logs, well cuttings and 3D pre-stack seismic data. Sequence stratigraphy techniques were applied in order to identify high-resolution depositional cycles that allow differentiating the vertical heterogeneity of this formation to the south of the Pottawatomie County. X-Ray Diffraction (XRD) analyses along with total organic carbon (TOC) analyses of well cuttings were combined with seismic attributes analysis and seismic inversion techniques to understand some physical characteristics of the rocks and their lateral distribution within each transgressive-regressive cycle. As a consequence, two prospective zones containing 1.46MMbls of oil-in-place in an area of approximately 260 acres has been identified after effectively integrating geological, geochemical and geophysical data.

Finally, a five-stage evolutional model is proposed for the study area where incised valley development, karstification and the progressive collapse of carbonate-dissolution features on the underlying Hunton unconformity surface enhanced the accommodation space at certain locations and favored the deposition of thick and organic-rich strata of the Woodford Shale. These anomalous intervals with their contained organic content (TOC) can be mapped seismically, and illustrate the lateral, as well as vertical heterogeneity of strata in the study area.

CHAPTER 1: INTRODUCTION

The Woodford Shale is an organic-rich hydrocarbon source rock that extends across parts of West Texas, New Mexico, Kansas and Arkansas and covers almost entirely the state of Oklahoma. In the main oil-producing region of central and southern Oklahoma, 16 billion barrels of saturated hydrocarbons were estimated to have been expelled from these rocks (Comer, 1987).

The increasing interest in developing unconventional resources such as the Woodford Shale, has arisen in recent years due to the technological improvements in horizontal drilling, well completions and, not less importantly, to the high prices of liquid hydrocarbons in the international oil markets.

Over 1,500 wells have been drilled mostly in the Anadarko and Arkoma geologic basins, but the operators face a high risk when targeting this unconventional reservoir due to its high internal complexity and the fact that the organic material contained in these rocks is not fully understood (Woodford Oil Congress, 2014).

Intrinsic rock properties such as oil-generative organic matter, lithologic facies, rock density, rock velocity among others must be evaluated when studying an unconventional play in order to reduce the geologic risk of the identified prospects. In that sense, several technical studies and theses (referenced throughout this thesis) have been written over the last few years focusing on sequence stratigraphy, geochemical and

geomechanical characterization, fracture analysis, seismic interpretation and integrated reservoir characterization of the Woodford Shale in Oklahoma.

1.1 OBJECTIVES

The goal of this study is to develop an integrated characterization of the Woodford Shale in an area located in south-central Oklahoma in order to identify organic-rich prospective areas. For this purpose, a set of well logs (wireline and mudlogs) were used to build a high-resolution sequence stratigraphic framework to better characterize the Woodford's vertical heterogeneities whereas seismic inversion techniques, along with a multi-attribute analysis, allowed identifying lateral variations of some rock properties, including total organic carbon (TOC) content within the stratigraphic framework thus highlighting "sweet spots" that may have economic importance for hydrocarbons exploitation.

1.2 GEOLOGIC FRAMEWORK

1.2.1 Tectono-Stratigraphic Setting

Five sedimentary basins occur in Oklahoma: Anadarko, Ardmore-Marietta, Hollis-Hardeman, Arkoma and the highly deformed Ouachita basin. The study area is located in the south part of the Cherokee Platform in Oklahoma (Figure 1.1). It is considered as an oil and gas province as part of the stable shelf area between the Arkoma

Basin and the Anadarko Basin and near the Criner Hills, Arbuckle Mountains, Hunton Arch, Nemaha Uplift, and the Nemaha and Central Oklahoma Fault Zones (Amsden, 1980; Campbell and Northcutt, 2001; Friess, 2005).

Figure 1.1 Geologic provinces in Oklahoma and study area for this research (modified after Johnson, 2008)

Precambrian and Cambrian igneous and metamorphic rocks are the oldest rocks in Oklahoma where the Reagan Sandstone was deposited after the first marine transgression during the Late Cambrian. It is overlain by thick limestones and dolomites of the Arbuckle Group. Simpson Group sandstones, Viola Formation limestones, and the Sylvan Shale are some of the most widespread marine rocks deposited during the Middle and Late Ordovician when Oklahoma had three major tectonic and depositional provinces: the Oklahoma basin, the southern Oklahoma aulacogen, and the Ouachita trough (Figure 1.2) (Northcutt et al., 2001; Johnson, 2008).

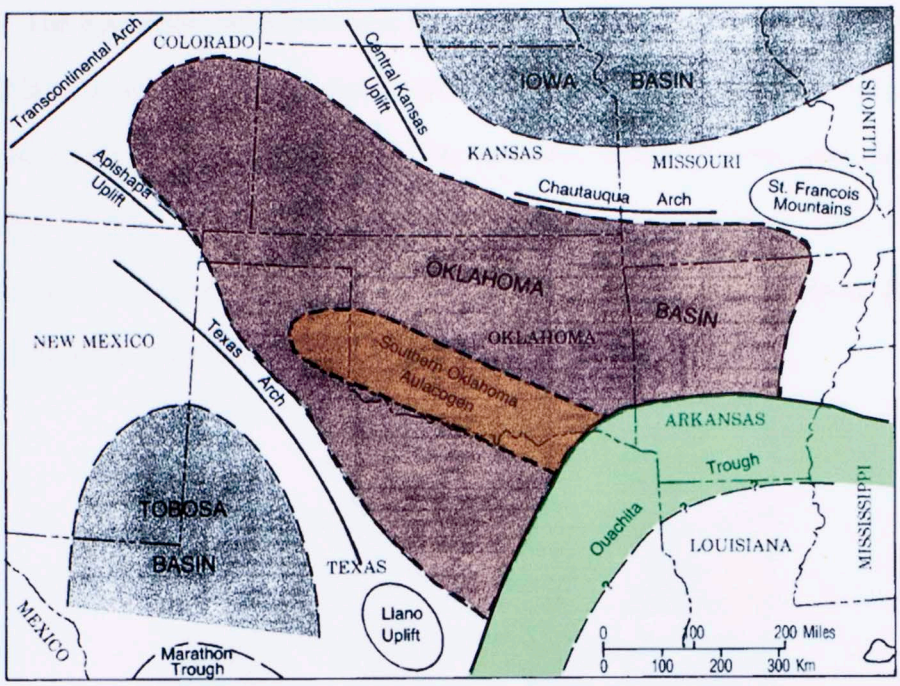

Figure 1.2 Map of southwestern United States showing approximate boundary of the three major depositional provinces in Oklahoma (modified after Campbell and Northcutt, 2001).

Limestones and dolomites of the Hunton Group were conformably deposited during the Late Ordovician-Early Devonian, followed by a period of widespread uplift and erosion that created a conspicuous unconformity that eroded from 500 to 1000 feet of strata, causing its dolomitization and karstification (Al-Shaieb et al., 2001; Johnson, 2008).

This dissolution and channeling event is recognized as the Middle to Late Devonian *pre-Woodford-Chattanooga unconformity* (Northcutt et al., 2001). The unconformity was subsequently buried under a blanket of transgressive black fine silt and clays of the Woodford-Chattanooga formations which covered most of the Oklahoma basin.

The Sycamore and Mississippi limestones and cherts dominate the sedimentary record in most areas as shallow seas covered most of Oklahoma during the Mississippian time. Nevertheless, rapid subsidence of the southern Oklahoma aulacogen resulted in deposition of the Caney, Goddard and Springer Shales (Northcutt et al., 2001; Johnson, 2008). Figure 1.3 illustrates a generalized stratigraphic column highlighting the most relevant Silurian-Mississipian stratigraphic units in the Anadarko Basin.

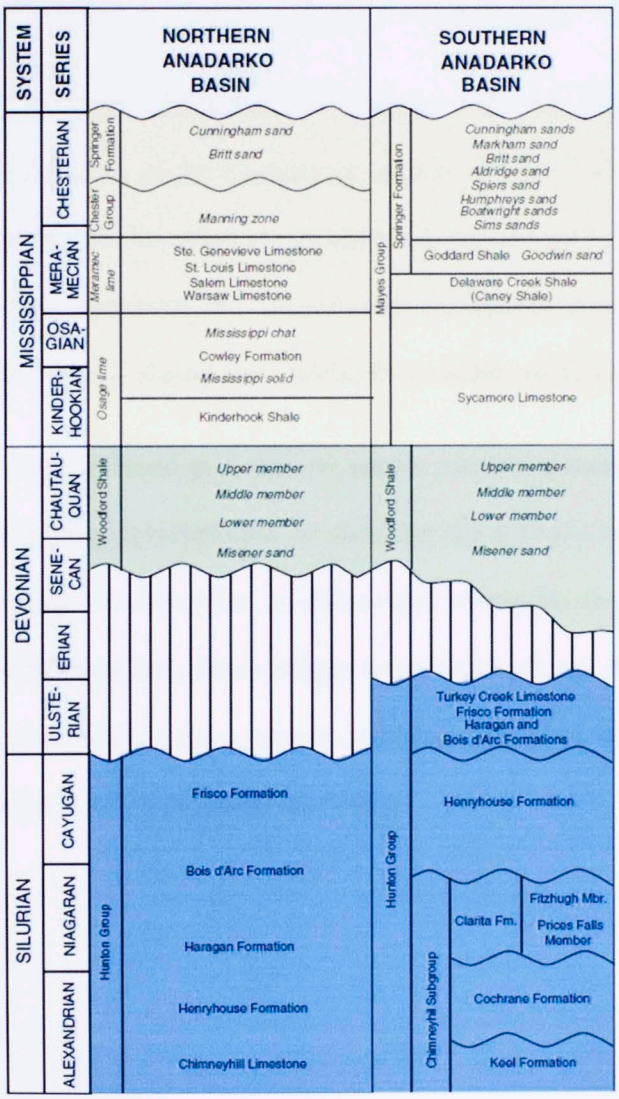

Figure 1.3 Generalized stratigraphic column for the Anadarko Basin (modified from Henry and Hester, 1995)

Orogeny and basin subsidence in the south along with a raise of broad areas in the north, characterize the Pennsylvanian period in Oklahoma where marine shales, beds of coal, conglomerates, sandstones and limestones were extensively deposited, thus generating the most important conventional hydrocarbon reservoirs (Johnson, 2008).

1.2.2 The Devonian Woodford Unconventional Resources Play

In the Late Devonian, Oklahoma, New Mexico and some parts of Texas, were located within 5° to 15°south of the Fammenian equator (Figure 1.4) where the humid climate favored a salinity stratification of the water column that led to anoxic conditions on the sea floor, thus permitting the preservation of organic matter in a reducing environment (Comer, 1991; Kirkland et al., 1992; Kuykendall and Fritz, 2001).

During this time, a broad and shallow epeiric sea transgressed from the south south-east over an irregular low-relief cratonic shelf that did not have significant orogenic barriers, thus preventing the deposition of deltaic and submarine-fan deposits. Storms probably were more frequent and able to trigger some bottom flows, but rising sea level and stable climatic and oceanographic patterns allowed deposition of thick mudstones (Comer, 1991; Sullivan, 1985; Kirkland et al., 1992).

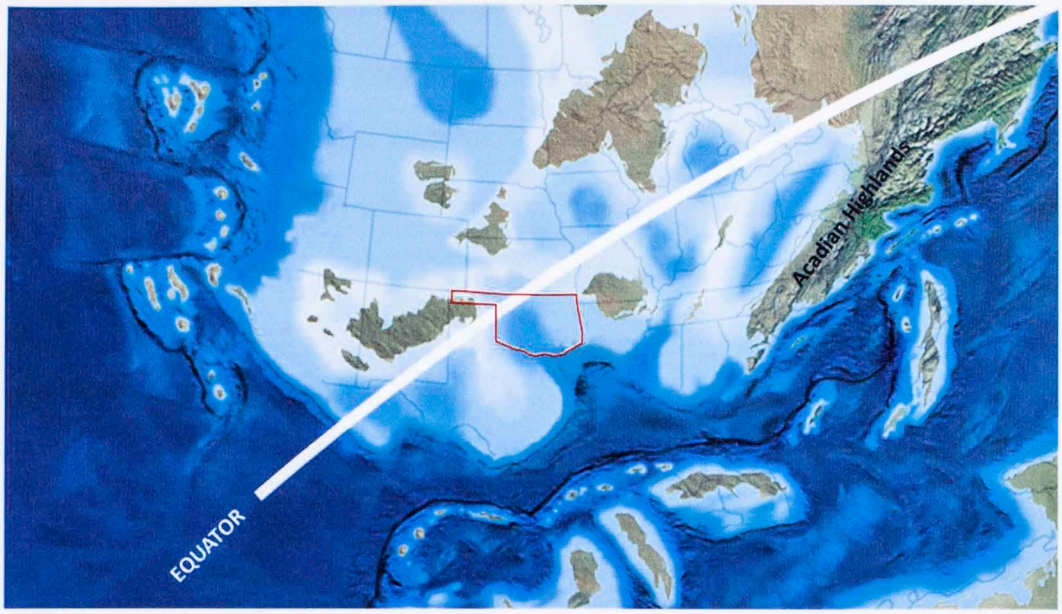

Figure 1.4 Paleogeographic map of United States highlighting the location of Oklahoma in the Late Devonian (360 m.a) (modified from Kirkland et al., 1992 and Blakey, 2014)

The Woodford Shale (Upper Devonian-Lower Mississippian) was deposited mainly upon the Hunton Group unconformity, although in some areas, the shale overlies older sediments. Thus, the lower boundary of the Woodford, and its stratigraphic equivalents, represents a major regional unconformity that extends across the southern mid-continent and records a major period of uplift and erosion. It is overlain by the glauconitic shaly Sycamore Limestone (basal part of the Mississippian Mayes Group) representing only a minor stratigraphic break which is disconformable only at some localities (Sullivan, 1985; Comer, 1991).

The dominant Woodford lithology is black shale, but chert, siltstone, sandstone, dolostone, and light-colored shale are locally common. In general, proximal lithofacies and basin depocenters contain more silt and sand and distal lithofacies contain more chert. The highest concentrations of organic carbon are found in intermediate settings remote from clastic source areas and it is typically 50 to 200 feet thick although it can reach up to 600 feet in thickness in the Arbuckle Mountains (Comer, 2007; Johnson, 2008).

In some areas, especially in north-central Oklahoma, the Woodford overlies a well-developed dolomitic sandstone known as the Misener Sandstone, composed of detrital quartz grains set in a matrix of crystalline dolomite and interpreted as a shoreline deposit (Amsden and Klapper, 1972) or a basal incised valley fill (Slatt, pers. comm., 2014)

Several studies (Cardott and Lambert, 1985; Lambert, 1992; Comer, 2008) have demonstrated that a mixture of Types I, II and III kerogen is found in the Woodford Shale. Organic carbon content ranges 0.5 - 28% with a thermal maturity closely related to local structure.

The highest maturity is reached in the Anadarko and Arkoma basins where the Woodford is deeply buried. Thus, in deep basins, the Woodford is in the gas window whereas in the shelf and platforms, as well as in the shallower parts of basins, it is in the oil window (Figure 1.5) (Comer, 2008).

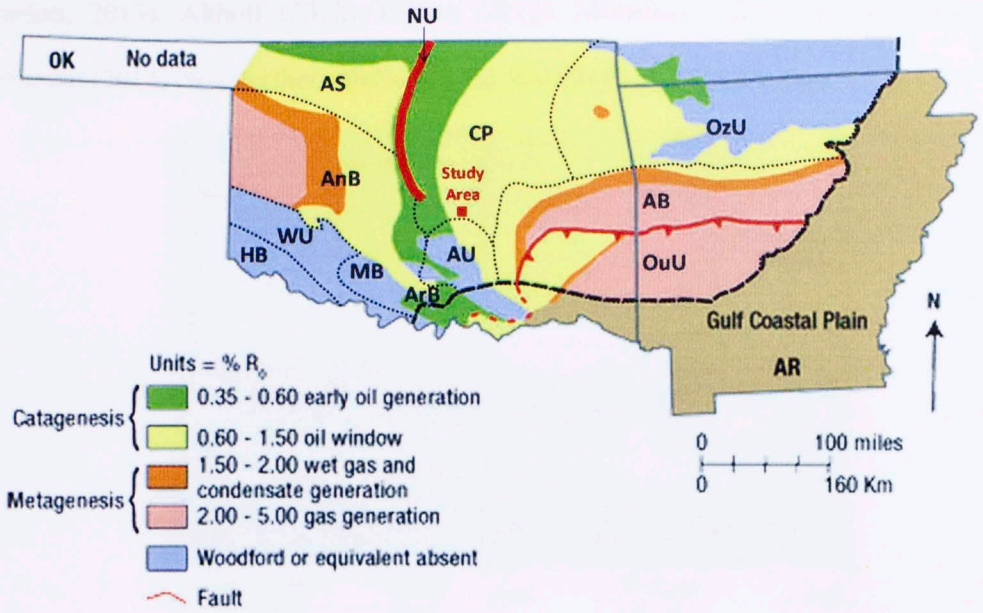

Figure 1.5 Thermal maturity map of the Woodford Shale in Oklahoma (OK) and Arkansas (AK) based on vitrinite reflectance values (%Ro) with outlines of the major geologic provinces (dashed lines) (modified from Comer, 2008). Abbreviations: AB=Arkoma Basin, AS=Anadarko Shelf; AnB=Anadarko Basin, AU=Arbuckle Uplift, ArB=Arbuckle Uplift, CP=Cherokee Platform, HB=Hollis Basin, MB=Marietta Basin, NU=Nemaha Uplift, WU=Wichita Uplift, OoU=Ouachita Uplift, OzU=Ozarka Uplift.

Considering eustatic sea level fluctuations, the Woodford Shale is defined as a second-order transgressive sequence with superimposed third-order (and most likely fourth-order) fall-rise cycles (Slatt, 2013; Houseknecht et al., 2014).

Three informal members (Lower, Middle and Upper) have been recognized in the Woodford based upon lithologic changes, palynology assemblages, organic geochemistry, well log response and, chemostratigraphy within the context of a sequence stratigraphic framework (Figure 1.6) (Lambert, 1992; Slatt and Rodriguez, 2012;

Cardott, 2013). Althoff (2012), Killian (2012), Molinares (2013), Serna (2013), and Tréanton (2014) have further subdivided the Woodford in different areas.

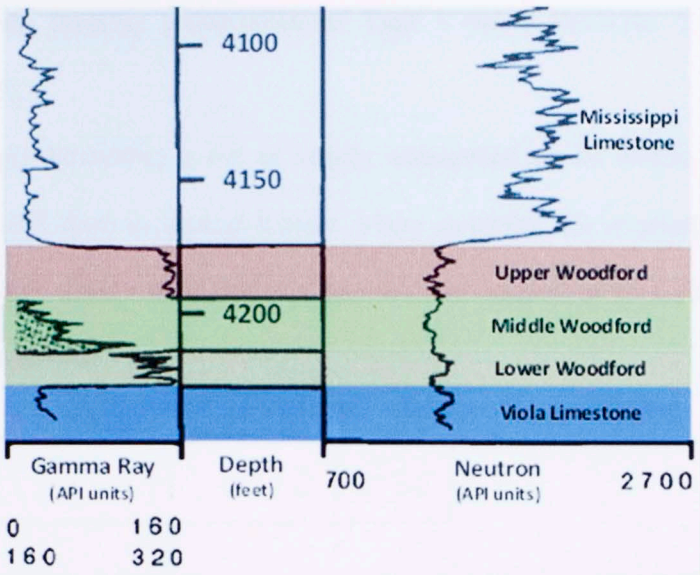

Figure 1.6 Informal members of the Woodford Shale according to well logs response (modified from Lambert, 1992)

The Lower Woodford is the least areally widespread of the three members, being thicker in the Oklahoma aulacogen (about 150 feet). It is characterized by regressive and transgressive gamma-ray log hemicycles and composed of laminated argillaceous organic-rich mudstones. A high concentration of pollen and spores suggests deposition close to shorelines in a progressive transition from a weakly to moderately restricted basin (Lambert, 1992; Molinares, 2013; Treanton, 2014).

The Middle Woodford has the largest lateral extent, reaching a thickness of 200 feet in the Iowa basin of eastern Kansas; although it is much thicker in southern Oklahoma. To the north, it is composed of dolomite and limestone suggesting deposition in a relatively shallow depositional environment (Lambert, 1992). In central Oklahoma, more finely laminated argillaceous mudstones with phosphate nodules were preserved.

There, Treanton (2014) has observed a decrease in clastic content along with increasing biogenic silica suggesting more marine conditions in an increasingly reducing environment, thus favoring preservation of Type I and II kerogens (Lambert, 1992; Molinares, 2013).

The Upper Woodford is not as areally widespread as the middle member. It is thickest (about 150 feet) in central Kansas where dolomite silt is abundant (Lambert, 1992). Nonetheless, finely laminated argillaceous and calcareous mudstones prograded across central Oklahoma.

CHAPTER 2: DATA SET AND METHODS

The study area is located in Pottawatomie County in south-central Oklahoma (Figure 2.1) which sits in the south part of the Cherokee Platform geologic province where the Woodford Shale can be found between 3050 to 3300 feet below surface with an average thickness of 180 feet. In this province, Amorocho (2012) developed stratigraphic and seismic studies to characterize the heterogeneities of the Woodford Shale.

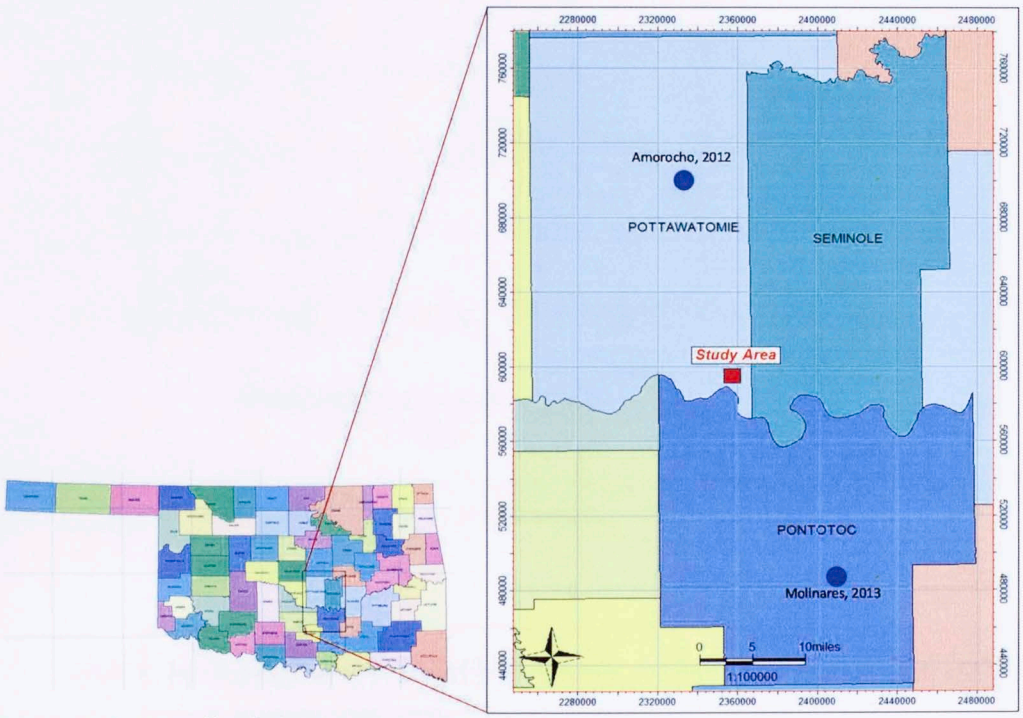

Figure 2.1 Detail of the location of the study area in Oklahoma.

11 The available data for this present study is composed by a 3D pre-stack, time migrated seismic survey that covers an approximate area of 2 square miles as well as digital or raster wireline logs for 13 vertical wells that penetrated the Woodford Shale (Figure 2.2).

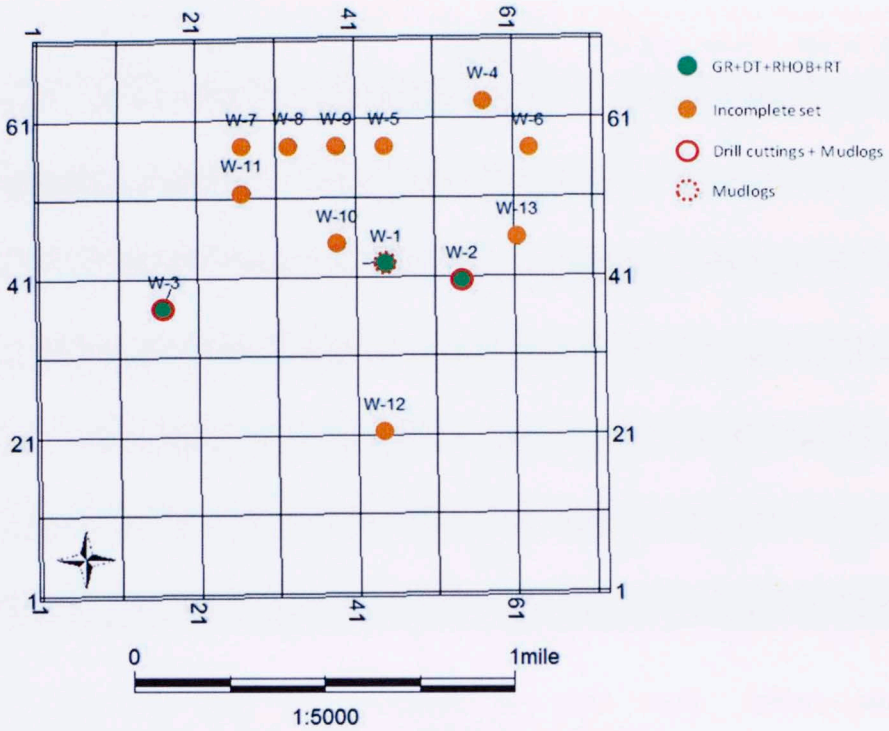

Figure 2.2 3D seismic survey and well locations colored according to the type of logs available for the Woodford Shale.

As it is not uncommon in subsurface studies, a substantial part of this group of wells does not have a comprehensive and complete set of wireline logs. Spontaneous potential (SP), resistivity (RT) as well as a few gamma-ray (GR), density (RHOB) and sonic (DT) logs were the most common logs available. Nevertheless, being that the Woodford Shale is a highly radioactive source rock, most of the recorded gamma-ray

readings were above 150 GAPI units and therefore plotted out-of-scale in the gamma-ray log, making it difficult to impossible to recognize lithological variations within the formation. Table 2.1 summarizes the kind of logs that were available for each well along with its format and relative quality.

Well	Digital or Raster file	Quality	Gamma-ray	Spontaneous Potential	Density	Sonic	Resistivity
W-1	D	Good	Yes	Yes	Yes	Yes	Yes
W-2	D	Good	Yes	Yes	Yes	Yes	Yes
W-3	D	Good	Yes	Yes	Yes	Yes	Yes
W-4	D	Poor	Inc	No	Inc	Yes	Yes
W-5	R	Poor	OOS	No	Yes	No	Yes
W-6	R	Poor	OOS	No	Yes	No	Yes
W-7	D	Poor	No	Yes	No	No	Yes
W-8	R	Poor	OOS	No	Yes	No	Yes
W-9	R	Poor	Inc	No	No	Yes	Yes
W-10	R	Poor	OOS	No	No	No	Yes
W-11	R	Poor	No	Yes	No	No	Yes
W-12	R	Poor	No	Yes	No	No	Yes
W-13	D	Poor	Yes	No	Inc	Yes	No

Table 2.1 Wireline logs set available for this study. Abbreviations: D=Digital, R=Raster, Inc=Incomplete, OOS=Out-of-scale

Not surprisingly, the most complete logs set was acquired in wells W-1, W-2 and W-3 that were drilled between 2010 to 2012 to produce hydrocarbons from the Hunton Group and Viola Formation. Therefore fairly good quality of information was preserved and used in this characterization study.

Well logs from these three wells were used to build a high-resolution sequence stratigraphic framework and also as input for the seismic-well tie and the qualitative and quantitative seismic interpretation aiming to define geologic structural features.

Drill cuttings from well W-2 were used to analyze rock composition through X-Ray Diffraction (XRD) analysis as well as organic-richness and thermal maturity through Rock-Eval testing. Unfortunately, those samples from well W-3 did not have the required amount of material to run the same kind of analyses. However, this pitfall did not prevent using the geochemical results to calibrate total organic carbon (TOC) content logs obtained after applying the delta-log R technique of Passey (1990) to analyze the variations of organic-richness across different beds of the Woodford Shale.

These calibrated organic-richness logs were further used as a training dataset in a multi-linear regression algorithm to predict TOC based on seismic data to identify prospective zones.

CHAPTER 3: SEQUENCE STRATIGRAPHY

Sequence stratigraphy is a methodology that provides a framework for any depositional setting, facilitating the prediction of facies and lithologies by relating changes in stratal stacking patterns to responses in changing accommodation and sediment supply through time, providing a context to interpret the spatial and temporal evolution of depositional systems (Cantenau et al., 2011).

Posamentier and James (1993) highlight that not only relative sea-level changes, but also sediment flux and physiography are the primary controls on the stratigraphic succession in the geologic record.

The recognition of condensed sections (highly radioactive or organic-rich shales), maximum flooding surfaces (mfs) along with sequence boundaries (unconformities or their correlative conformities) is the essential starting point to develop a sequence stratigraphy interpretation.

A stratigraphic sequence includes two or more systems tracts (ST) deposited during certain eustatic sea level stages in a full transgressive-regressive (T-R) cycle. When relative sea-level falls, shorelines move seaward, eroding sediments from the shelf towards the basin and creating major unconformities or sequence boundaries (SB). These deposits seaward of the shoreline are named falling stage systems tracts (FSST) implying that they were deposited during a falling stage of relative sea level. When sea level starts to raise, shoreline erosion may occur, creating a transgressive surface of erosion (TSE)

which is the upper boundary of FSST deposits. Sea level continues rising and progressively moves the shoreline landward allowing the deposition of transgressive systems tracts (TST) up to a maximum flooding point where a maximum flooding surface (mfs) is created and constitutes the upper boundary of the TST. Highstand system tracts (HST) are deposited during a slowdown of the rate of rising sea level where the accommodation space begins to be sediment-filled, moving the shoreline seaward (Figure 3.1) (Mitchum, 1977; Vail et al., 1977; Van Wagoner et al., 1990; Posamentier, and James, 1993; Cantenau et al., 2011).

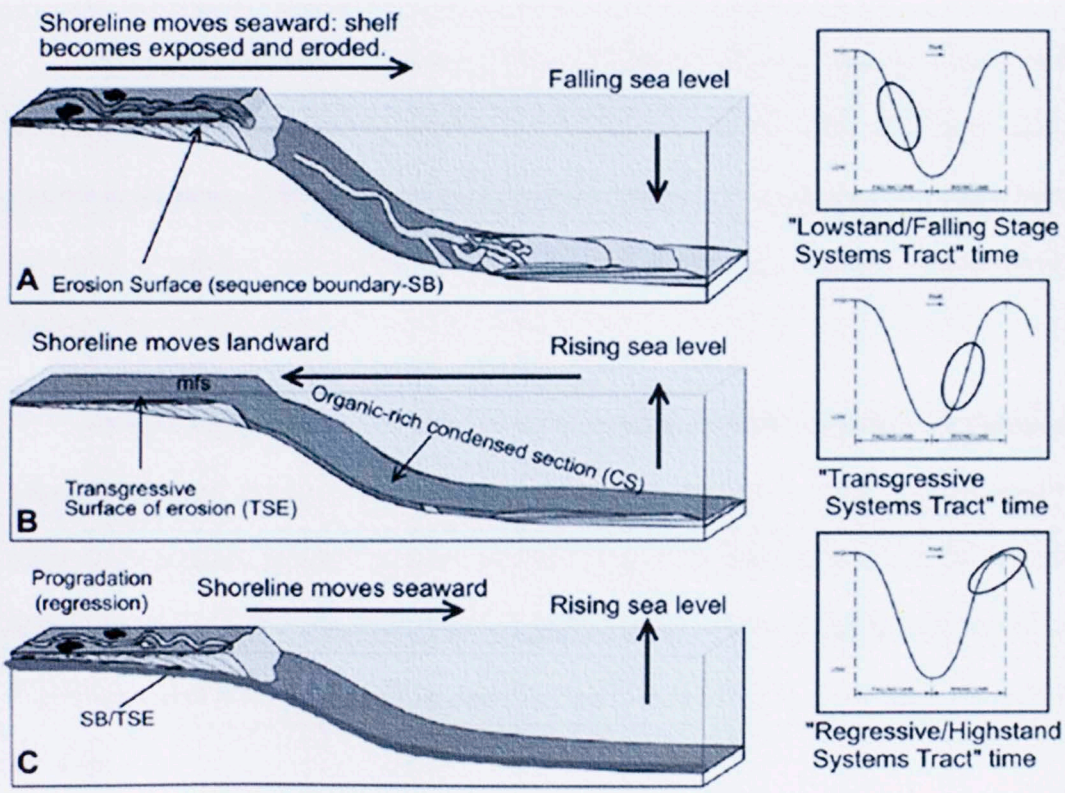

Figure 3.1 Schematic description of the evolution of sequence stratigraphic system tracts during (a) a relative sea-level fall, (b) a relative sea-level rise (transgression), and (c) a relative slowdown in the rate of sea-level rise (progradation) (Slatt and Rodriguez, 2012).

These sequence stratigraphy concepts can be applied to understand and predict vertical and lateral heterogeneities of organic-matter-rich rocks (ORRs), but also require considering the physiographic setting where they accumulated: constructional shelf margin, platform/ramp or continental slope/basin, as they control the production, destruction and dilution of the organic-matter (Bohacs et al., 2005; Passey et al., 2010).

An upward shoaling package of genetically related beds and bedsets is defined as a *parasequence*. It is the essential building block to understand stratigraphic controls and architectures of ORRs (Passey et al., 2010).

The Woodford Shale, deposited over a time span of 33 m.a, has been interpreted as a second-order depositional sequence comprised of several third (and most likely fourth) order parasequences that bring a complex lithofacies distribution associated with variations in palynology, organic geochemistry and electric log response (Gupta, 2012; Cardott, 2013: Slatt, 2013).

In this study, a based-on-gamma ray log, high-resolution sequence stratigraphy interpretation was carried out for the Woodford Shale by identifying its second-order sequence boundaries (Top of Hunton Group and Top of Woodford Shale) and its internal higher-frequency T-R cycles represented as parasequences. The tops of Sylvan and Viola Formations were also interpreted in order to analyze variations in gross thickness across the area.

Amorocho (2012) described in detail the qualitative response of different logs in the above mentioned stratigraphic units for a reference well located 20 miles to the northwest of the present study area (Table 3.1)

Stratigraphic Unit	Gamma Ray	Resistivity	Velocity
Woodford Shale	High	High	Low
Hunton Group	Low	-	High
Sylvan Shale	High	Low	-
Viola Formation	Low	High	High

Table 3.1 Qualitative response of certain well logs for different stratigraphic units in the Cherokee Platform.

Even though some of the wells in the study area do not have a complete and uniform set of logs, the same distinctive behavior was observed and allowed the interpretation of the relevant stratigraphic markers in the available wells (Figure 3.2)

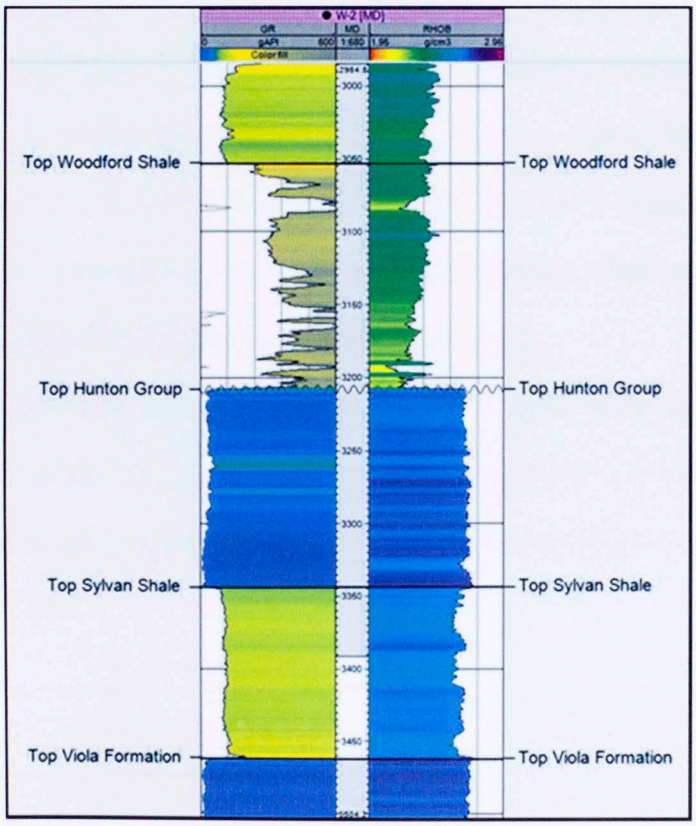

Figure 3.2 Type log for well W-2 depicting the well log response of the Woodford Shale, Hunton Group, Sylvan Shale and Viola Formation.

3.1 INTRA-WOODFORD TRANSGRESSIVE-REGRESSIVE CYCLICITY

A gamma-ray log is the fundamental tool to differentiate lithologies owing to its sensitivity to the natural occurrence of radioactive components of different minerals and total organic carbon content (TOC) in rocks. High concentrations of quartz and carbonates tend to decrease the API readings of the gamma-ray tool but conversely, high concentrations of clays and organic-matter tend to increase them.

Other tools such as density and sonic logs can also be used as proxies for lithological interpretation in unconventional reservoirs as the presence of organic-matter content reduces the density and the P-wave velocity of the rock (so does porosity).

Amorocho (2012) identified ten parasequences in a study area in the central Cherokee Platform categorizing gamma-ray patterns (high API readings upward, low readings upward or constant readings upward) as recognition criteria for revealing the vertical heterogeneity of the Woodford Shale (Appendix A).

Out of the thirteen wells available for this study, three of them had a good enough log quality to construct a higher-resolution sequence stratigraphy framework composed of ten parasequences (PS) after identifying their upward coarsening or upward shoaling patterns (Figure 3.3).

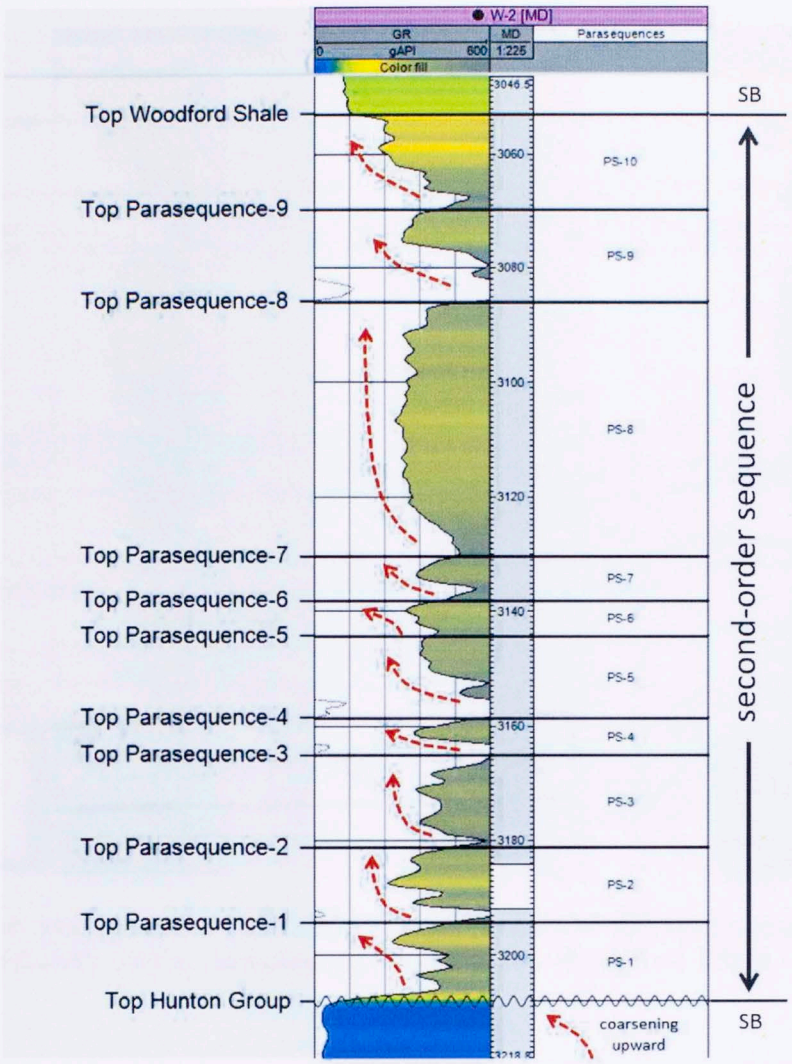

Figure 3.3 Gamma-ray log of well W-2 showing the second-order sequence boundaries (SB) of the Woodford Shale and its over-imposed parasequences.

A local well correlation reveals good lateral continuity of all of the interpreted parasequences and exhibits almost the same gross thickness and distinctive stacking patterns except for the lowermost three basal parasequences which show variation in thickness and composition (Figure 3.4).

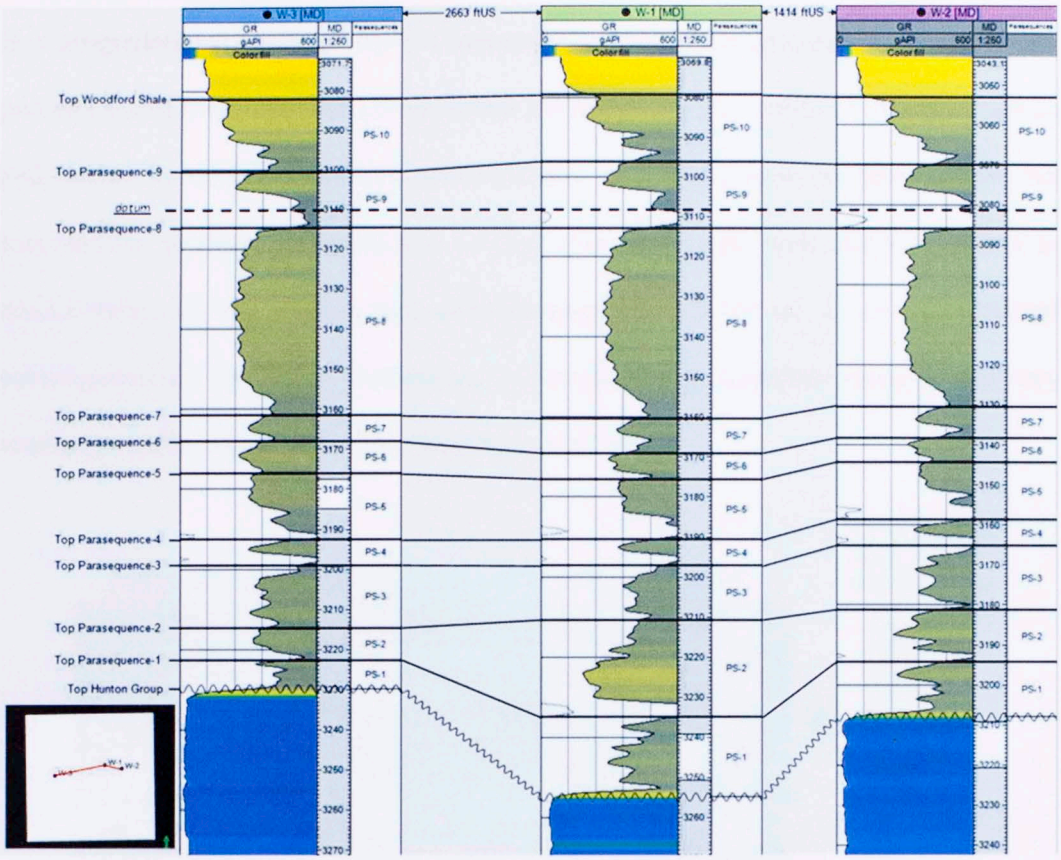

Figure 3.4 Stratigraphic well log correlation across the study area showing lateral continuity of the parasequences within the Woodford Shale.

A succession of genetically related parasequences forming a distinctive stacking pattern and bounded by flooding surfaces (*fs*) and/or their correlative surfaces is defined as a *parasequence set* (Van Wagoner et al., 1990; Vail, et al., 1977; Mitchum, 1977; Posamentier and James, 1993).

Three types of parasequence sets can be identified based on their stacking pattern: In a progradational parasequence set successively younger parasequences contain higher percentages of rocks deposited in shallower environments than underlying parasequences and tend to be thicker than older parasequences. In a retrogradational parasequence set successively younger parasequences contain more shale and more rocks deposited in deeper-water, and are thinner than older parasequences in the set. In an aggradational parasequence set the facies, thicknesses, and sandstone to mudstone ratios do not vary stratigraphically (Figure 3.5) (Van Wagoner, et al., 1990).

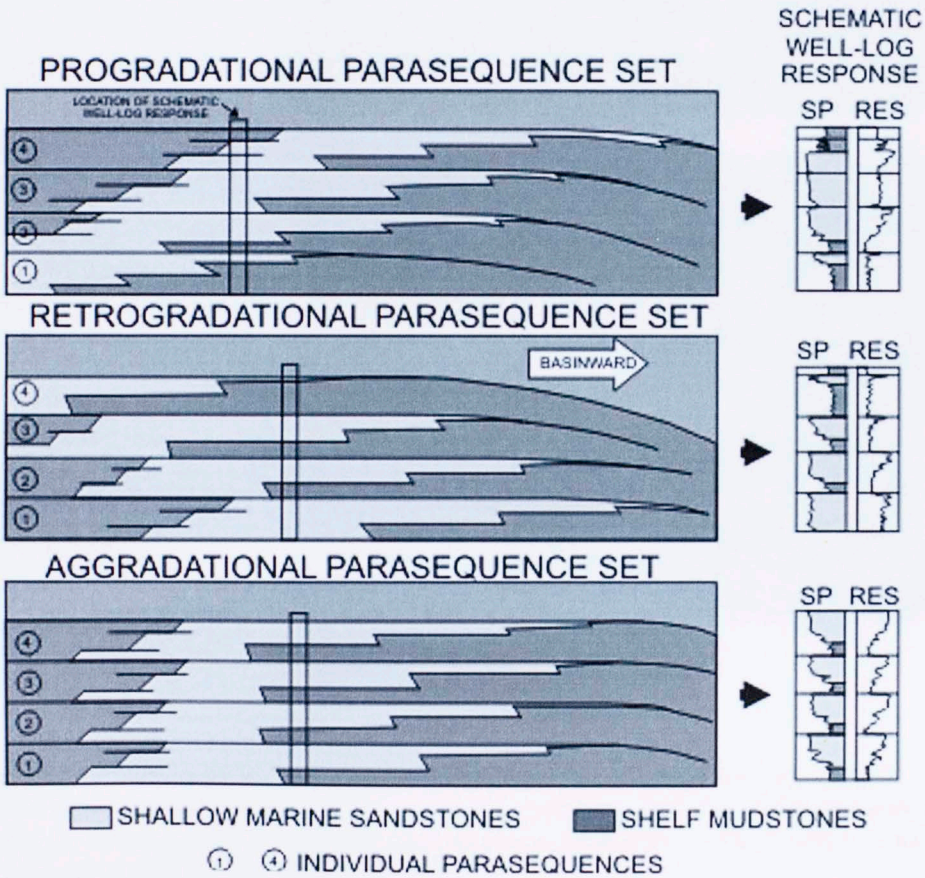

Figure 3.5 Parasequence-stacking patterns in parasequence sets (from Van Wagoner et al., 1990).

According to vertical stacking patterns differentiation, four parasequence sets are proposed in this study as main constituents of the Woodford Shale.

The basal Parasequence Set A (PSS-A) groups PS- 1 to PS-4 and can be categorized as retrogradational with high variations in thicknesses (from 35 to 60 feet) (Figure 3.6). Deposition was during the first pulse of transgressive sediments that back-filled the structural lows and erosional features carved out by the post-Hunton marine regression; especially PS-1 and PS-2. PS-3 and PS-4 seem to be deposited over a more evenly shaped surface (Figure 3.4).

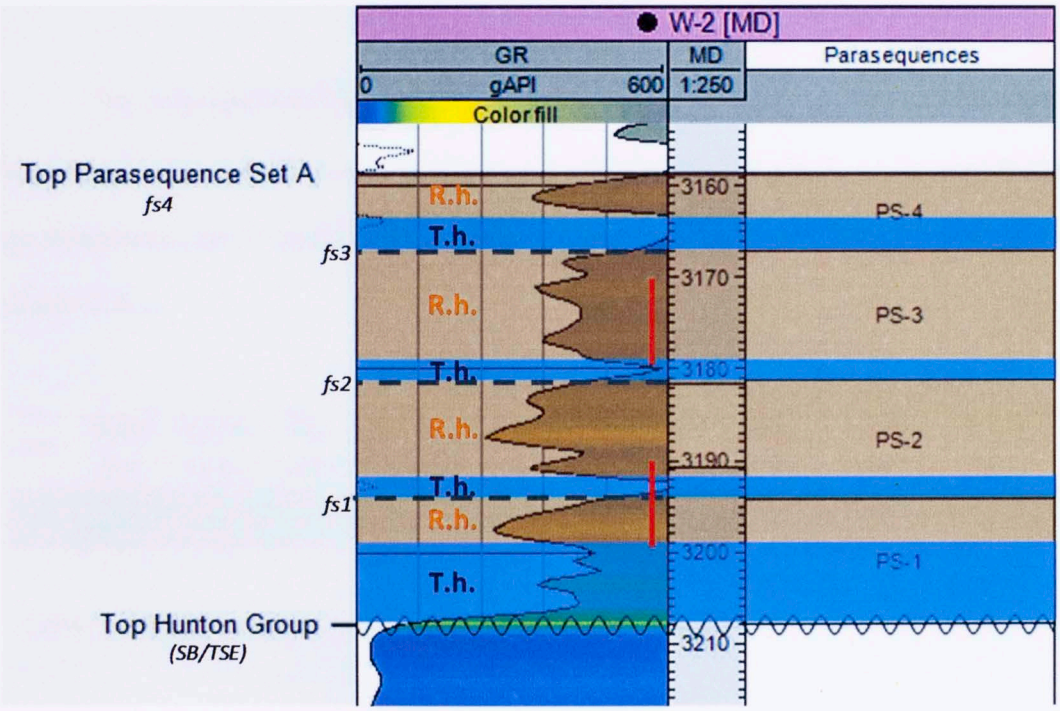

Figure 3.6 Parasequence Set A of the Woodford Shale showing a generalized aggradational-to-retrogradational stacking pattern and the transgressive and regressive hemicycles (T.h/R.h) of each parasequence. Red lines represent locations of cuttings for XRD analyses.

According to X-Ray Diffraction (XRD) analyses, two cutting samples taken from PS-2 and PS-3 in well W-2, are composed mainly by quartz and illite/mica with minor proportions of kaolinite, dolomite and plagioclase (Table 3.2)

PS	Depth (feet)	Quartz (wt%)	Illite (wt%)	Kaolinite (wt%)	Dolomite (wt%)	Plagioclase (wt%)	Feldspar (wt%)	Calcite (wt%)	Pyrite (wt%)
2	3190-3200	54	33	5	3	2	1	1	1
3	3170-3180	56	28	6	3	3	1	1	2

Table 3.2 Mineralogical composition of some parasequences of the Parasequence Set A.

The progradational Parasequence Set B (PSS-B) encompasses PS-5 and PS-6 and is around 20 feet thick (Figure 3.7). The composition of PS-5 is similar to the underlying parasequences, but it contains less quartz compensated by more dolomite and pyrite (Table 3.3).

PS	Depth (feet)	Quartz (wt%)	Illite (wt%)	Kaolinite (wt%)	Dolomite (wt%)	Plagioclase (wt%)	Feldspar (wt%)	Calcite (wt%)	Pyrite (wt%)
5	3140-3150	53	31	5	4	3	1	1	2

Table 3.3 Mineralogical composition of Parasequence 5 of the Parasequence Set B.

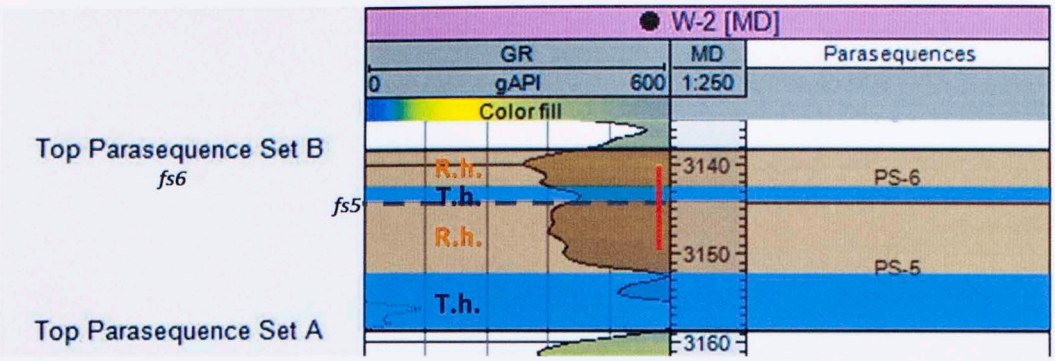

Figure 3.7 Parasequence Set B of the Woodford Shale showing a generalized progradational (coarsening upward) stacking pattern and the transgressive and regressive hemicycles (T.h/R.h) of each parasequence. Red line represents location of cuttings for XRD analysis.

Parasequence Set C (PSS-C) is around 50 to 60 feet in thickness (Figure 3.8). It encompasses PS-7 and PS-8 and exhibits a progradational stacking pattern suggesting a slow rise in sea-level. Drill cuttings taken from the upper part of PS-8 for XRD analysis reveals the presence of the same minerals found in the previous parasequence set but with a significant variation in their relative abundance, especially in quartz and illite/mica, and minor proportions of apatite (6%). (Table 3.4)

PS	Depth (feet)	Quartz (wt%)	Illite (wt%)	Kaolinite (wt%)	Dolomite (wt%)	Plagioclase (wt%)	Feldspar (wt%)	Calcite (wt%)	Pyrite (wt%)
8	3090-3100	61	19	4	3	2	1	1	2

Table 3.4 Mineralogical composition of Parasequence 8 of the Parasequence Set C.

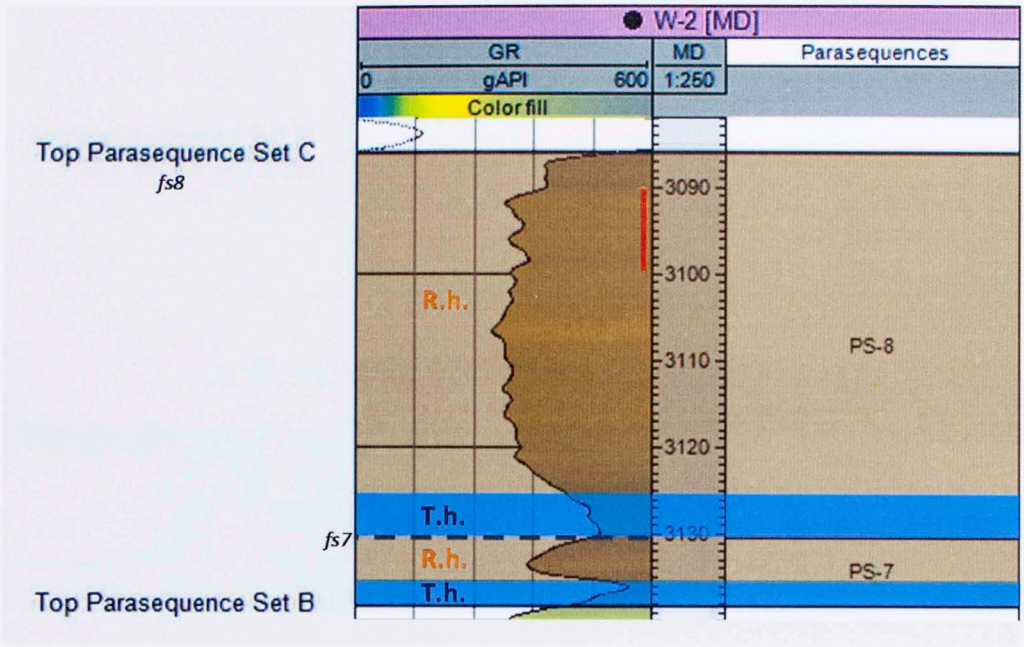

Figure 3.8 Parasequence Set C of the Woodford Shale showing a progradational-to-aggradational stacking pattern and the transgressive and regressive hemicycles (T.h/R.h) of each parasequence. Red line represents location of cuttings for XRD analysis.

The uppermost 30 feet of Parasequence Set D (PSS-D) tops the Woodford Shale and encompasses PS-9 and PS-10 (Figure 3.9). It shows a progradational stacking pattern suggesting a rising sea-level followed by an erosive period identified by Althoff (2012) in core observations and well logs.

Two samples taken of both transgressive and regressive hemicycles (T.h. / R.h.) of PS-9 highlight variations in its composition (Table 3.5)

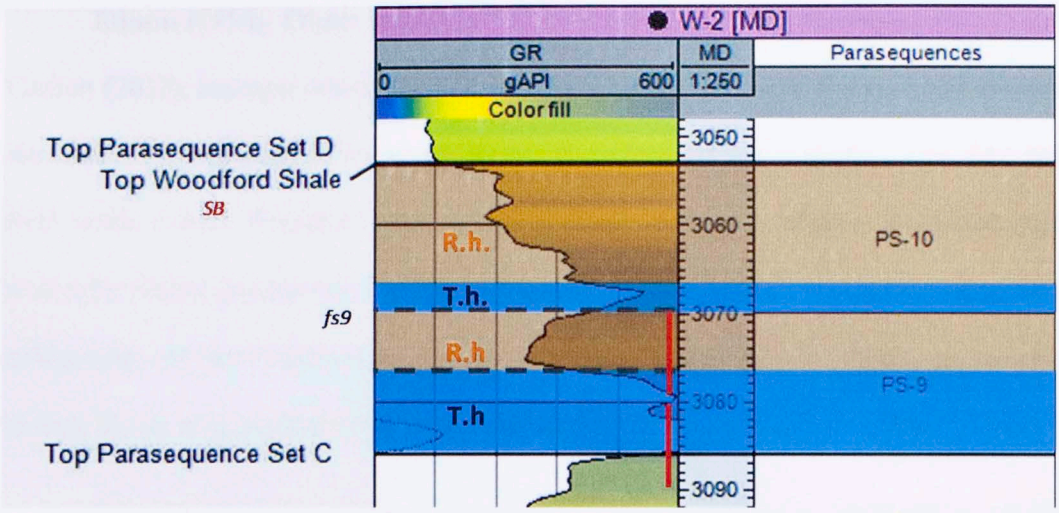

Figure 3.9 Parasequence Set D of the Woodford Shale showing a progradational stacking pattern and the sequence stratigraphic system tracts of each parasequence. Red lines represent locations of cuttings for XRD analyses.

PS	Depth (feet)	Quartz (wt%)	Illite (wt%)	Kaolinite (wt%)	Dolomite (wt%)	Plagioclase (wt%)	Feldspar (wt%)	Calcite (wt%)	Pyrite (wt%)
9	3070-3080	69	20	5	0	2	1	1	1
9	3080-3090	44	37	5	5	4	2	traces	3

Table 3.5 Mineralogical composition of Parasequence 9.

3.2 LITHOSTRATIGRAPHIC CORRELATIONS

Lithostratigraphy defines rock units based on the physical characteristics of rocks, whereas sequence stratigraphy defines them based on chronostratigraphy and focuses on the geologic significance of the surfaces that separate sedimentary successions (Posamentier and Allen, 1999).

Ellison (1950), Comer (1991) and more recently Slatt and Rodriguez (2012) and Cardott (2013), amongst others, have recognized that the Woodford Shale can be divided into three lithostratigraphic members, based on gamma-ray log response, core data and field work: Lower Woodford with relatively low gamma-ray, Middle Woodford with noticeably higher gamma-ray, and Upper Woodford with relatively low gamma- ray. This stratigraphy can be recognized not only in the geological provinces of Oklahoma, but also in west Texas, as described by Hemmesch et al. (2014).

Slatt and Rodriguez (2012) presented a lithostratigraphic subdivision of the Woodford Shale based on a sequence stratigraphic framework constructed for the Wyche Quarry well and correlated to the Henryhouse Creek Section described by Paxton et al. (2006) (Figure 3.10).

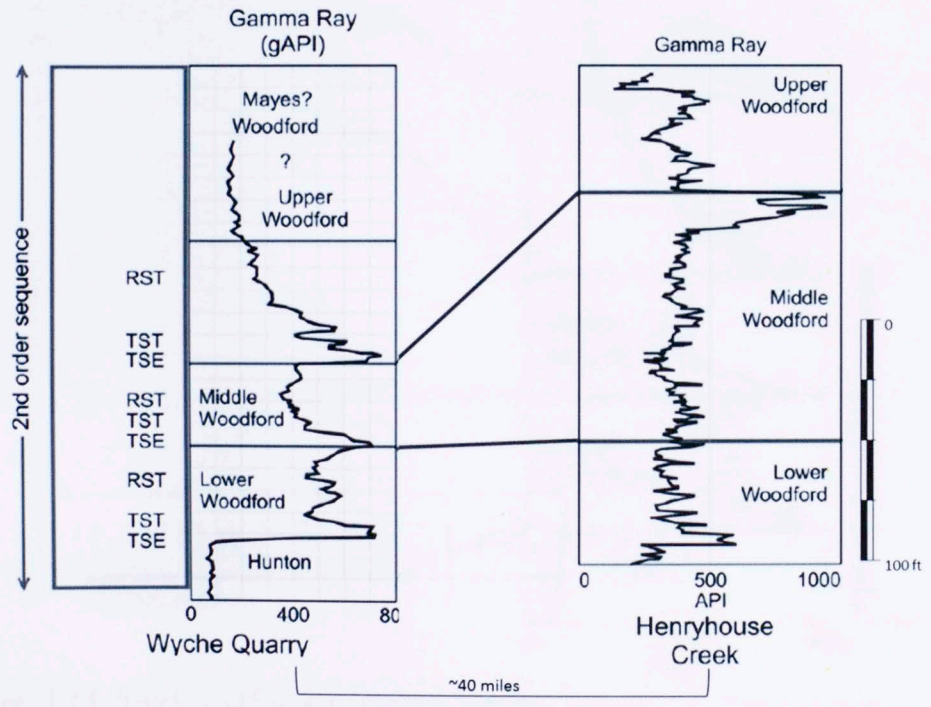

Figure 3.10 Correlation of the Woodford Shale from the Wyche Quarry and the Henryhouse Creek outcrop (modified from Slatt and Rodriguez, 2012)

These lithostratigraphic members have correspondence with the chronostratigrahic subdivision proposed in this study: Parasequence Set A (PS-1 to PS-4) is equivalent to the Lower Woodford and its retrogradational stacking pattern suggests that the accommodation space was progressively greater than the rate of sediment supply for this part of the basin. Prograding Parasequence Sets B and C (PS-5 to PS-8) are part of the Middle Woodford which was deposited under a quasi-steady sediment supply and relatively low sea-level fluctuations. Parasequence Set D (PS-9 and PS-10) forms the Upper Woodford that was deposited during a regressive stage (Figure 3.11).

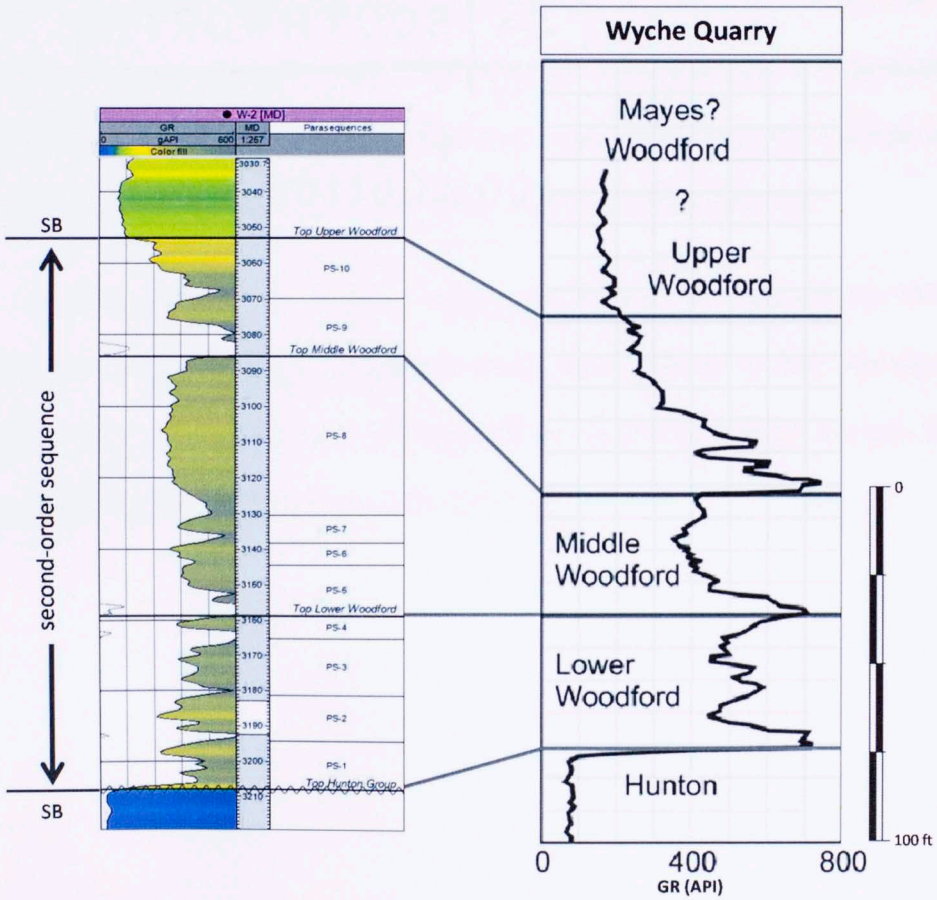

Figure 3.11 Stratigraphic correlation of the Woodford Shale between well W-2 and Wyche Quarry showing lithostratigraphic members and chronostratigraphic equivalences.

CHAPTER 4: SEISMIC ANALYSIS

Since the early 1990s 3D seismic has been a widespread tool used by geophysicists, geologists and engineers across the entire hydrocarbon exploration and production cycle. Its' benefits to the oil and gas industry are not only in providing better quality and resolution than its predecessor, 2D seismic, but also allowing complex subsurface structural delineation such as salt bodies, low angle faults and fractures. However, as current seismic data are generally limited to bandwidths from 10 to 70 Hz and unconventional reservoirs have thicknesses less than 400 feet, it is generally not possible to distinguish their internal architecture without further seismic analysis such as pre-stack and post-stack seismic inversion and seismic attribute extraction.

In this study, a 3D seismic volume acquired by the operator in 2010 was qualitatively and quantitavely interpreted using multi-attribute seismic analysis along with post-stack seismic inversion to recognize both major structural features and internal heterogeneities in the Woodford Shale (Figure 4.1).

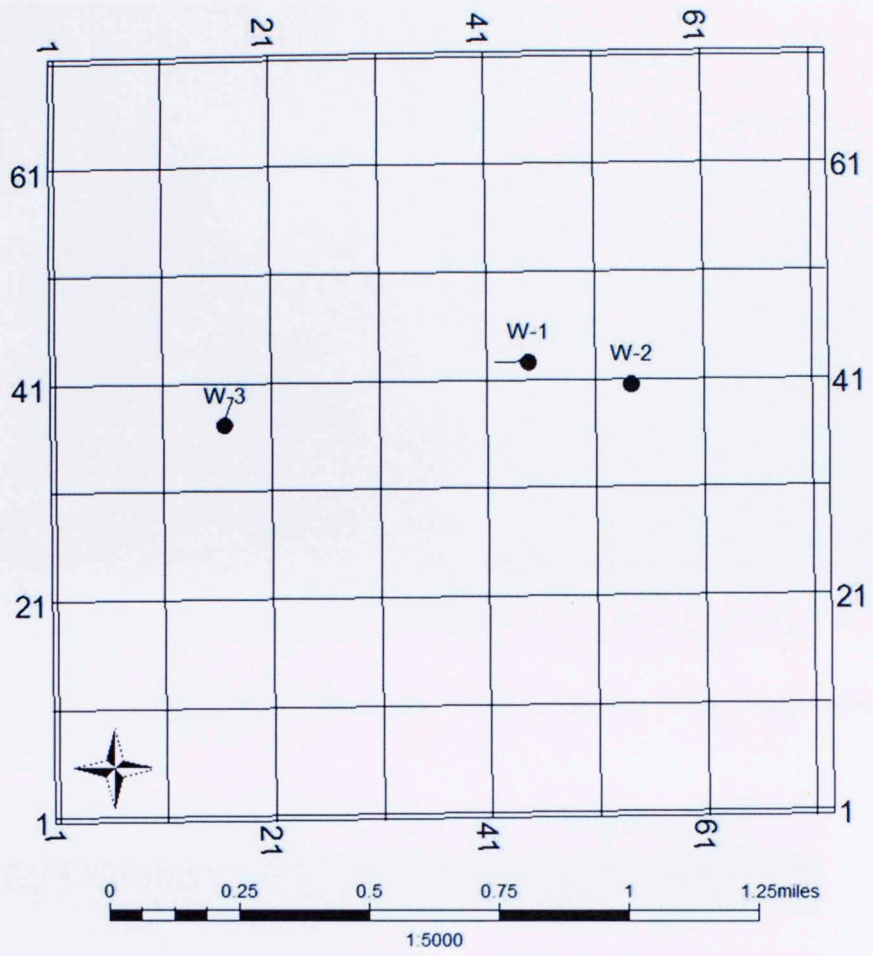

Figure 4.1 3D seismic survey and location of the wells with density and sonic logs used in the seismic interpretation.

Covering an area of approximately 2 square miles, the seismic volume analyzed and interpreted in this study is located in the south part of Pottawatomie Co, Oklahoma. Frequency content ranges from 4 Hz to 100 Hz (Figure 4.2). Acquisition parameters are summarized in Table 4.1.

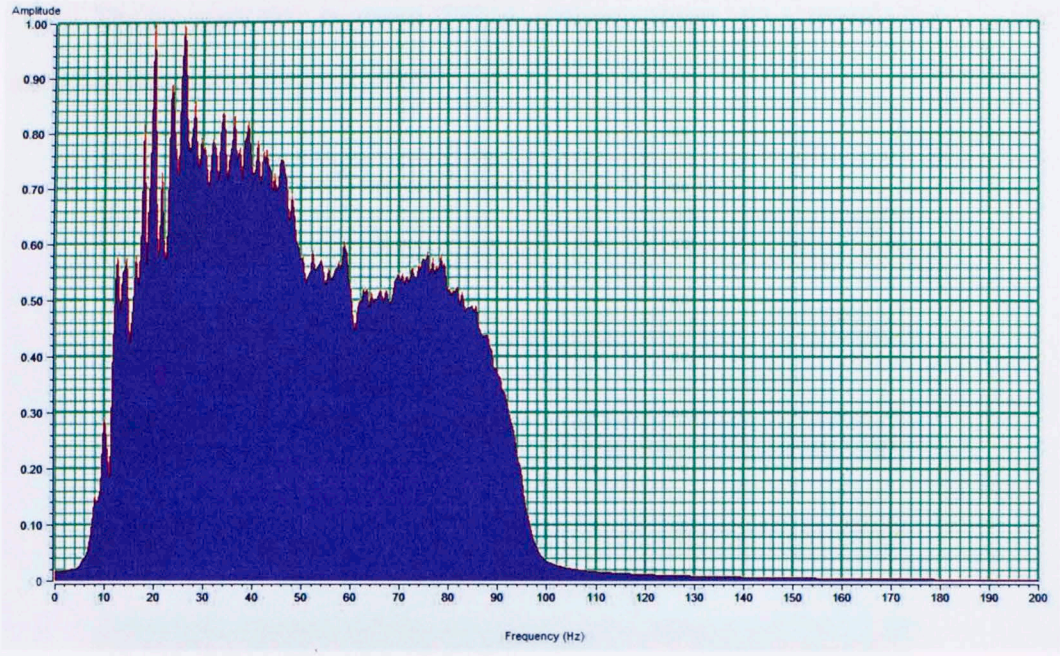

Figure 4.2 Frequency spectrum of the seismic survey in the study area.

Sample rate	1 millisecond
Record length	1.9 seconds
Distance between Inlines	110 feet
Distance between Xlines	110 feet
Inline direction	West-East
Xline direction	South-North
Range of Inlines	1-71
Range of Xlines	1-72
Azimuth	359.11

Table 4.1 Acquisition parameters of the seismic survey.

The pre-stack time migrated (PSTM) seismic volume was obtained after following the processing sequence described in Table 4.2.

Geometry assignment and Quality Control
Apply refraction statics – Shift to smooth floating datum
Edit traces and first break muting
Spherical divergence correction
Surface consistent decon (spiking, 160 ms operator)
Spectral whitening 5-100 Hz
Surface consistent scaling
Velocity analysis (0.5 mile spacing)
Auto-velocities (0.25 mile spacing)
Pre-stack Kirchhoff Time Migration
Residual velocity analysis (0.25 mile spacing)
Stack
Bandpass filter (6-96)
Trace envelope gain

Table 4.2 Processing history of the seismic survey.

The fundamental objective of the 3D seismic method is to increase resolution measured in terms of the seismic wavelength (λ) (Brown, 2004). However, geologic intervals cannot be resolved in seismic profiles if their thickness is less than a quarter of the seismic wavelength ($\lambda/4$).

In this seismic survey, the seismic wavelength in the Woodford Shale is around 20 milliseconds and averaged interval velocity is around 7150 feet/sec (Portas, 2009). Thus, beds thinner than 35 to 40 feet (5 milliseconds) are not resolved in amplitude seismic profiles.

4.1 SEISMIC-WELL TIE

In seismic surveying, seismic reflections occur at boundaries where there is a change in acoustic impedance regardless of changes in lithology. By using density and sonic logs, seismic interpreters can create synthetic seismograms in order to identify major stratigraphic tops in seismic profiles.

In the W-1 well, five stratigraphic units of interest were identified and a synthetic seismogram was created by using density and sonic logs to calculate reflection coefficients along its trajectory. These coefficients were convolved using a seismic wavelet extracted from the survey in a 200 millisecond window that included the top of the Mayes Formation to the top of the Hunton Group (Figures 4.3 and 4.4).

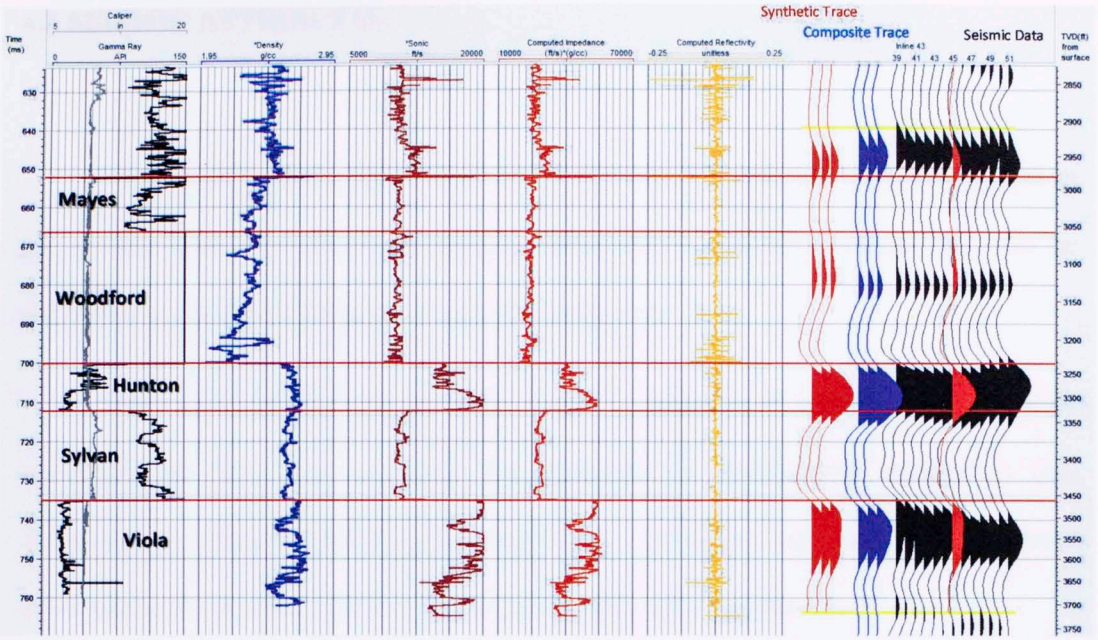

Figure 4.3 Synthetic seismogram for well W-1.

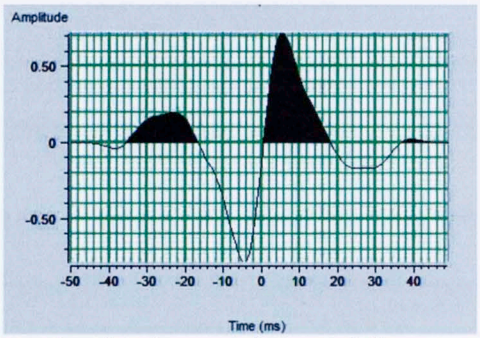

Figure 4.4 Extracted seismic wavelet used for convolution.

As a result of this process it was possible to establish the reflection character of different stratigraphic tops. Tops of the Hunton Group and the Viola Formation are both negative-to-positive zero crossings whereas the top of the Mayes Formation and the top of the Sylvan Shale are both positive-to-negative zero crossings. The top of the Woodford Shale is unidentifiable due to the lack of impedance contrast between this formation and the overlying lithologies.

4.2 SEISMIC ATTRIBUTES

A seismic attribute can be defined as any mathematical manipulation applied to the seismic data that allows the seismic interpreter to identify patterns that can be correlated to geological features or reservoir properties.

After their introduction in early 1970s, a plethora of seismic attributes were developed for two main purposes: (1) structural or stratigraphic delineation (i.e. instantaneous phase, instantaneous frequency, curvature, etc and (2) "indirect" hydrocarbon detection (AVO and reflection strength, amongst others).

In this study a seismic-attributes assisted interpretation of the Woodford Shale and Hunton Group provided not only a better structural interpretation of both units but also identification of potential prospective zones based on thickness variations.

The Attribute Assisted Seismic Processing and Interpretation Consortium (AASPI) of the University of Oklahoma has developed a state-of-the-science set of seismic attributes compiled in the AASPI proprietary software. Curvature and coherence (a.k.a. similarity or semblance) were calculated and analyzed for this particular dataset.

4.2.1 Curvature

Chopra and Marfurt (2007) have defined curvature in two dimensions as the radius of a circle tangent to a curve. In three-dimensions, two circles need to be tangent to the surface in order to mathematically describe its curvature.

Positive curvature is associated with domes or anti-form features whereas negative curvature is associated with syn-forms. Dipping planes will have zero curvature regardless of their dip angle (Figure 4.5).

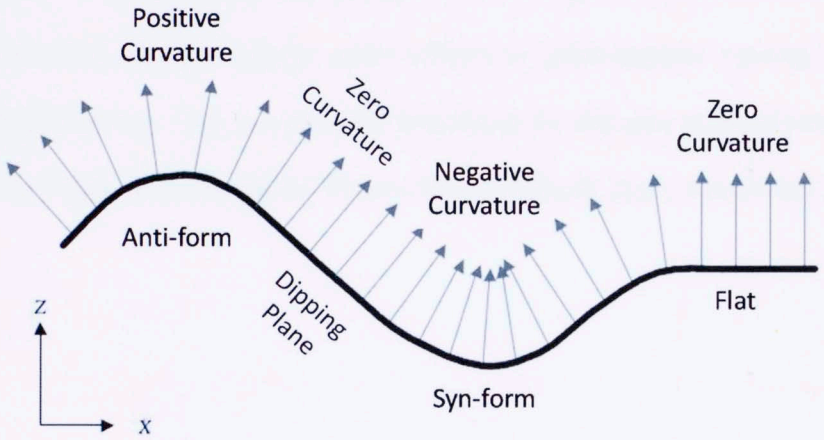

Figure 4.5 Illustration for curvature attributes (modified from Roberts, 2001). The arrows represent vector normal to the surface. Diverging vectors represent anti-forms and converging vectors represent syn-forms.

Curvature can be measured at any point and azimuth of a surface but only one of these azimuths will have the largest curvature and it is called *Maximum Curvature* and the curvature orthogonal to it is called *Minimum Curvature* (Klein et al., 2008).

The maximum and minimum curvature attributes can be confusing due to the amount of information contained within them. Most-positive and most-negative curvatures can be found by searching for all possible curvatures normal to the analyzed surface (Roberts, 2001).

The most-negative and most-positive curvatures are the most unambiguous of the curvature images in highlighting faults and folds (Chopra and Marfurt, 2007). Aiming to identify such particular structural features, both attributes were calculated and interpreted for the interval of interest.

Figure 4.6 shows a time slice through the most-negative curvature volume. Some observed dendritic patterns suggest paleo-valleys or paleo-streams running across an irregular ridged surface. This is a plausible hypothesis for this area as some workers have reported dissolution structures in the Hunton Group (Althoff, 2012; Amorocho, 2012).

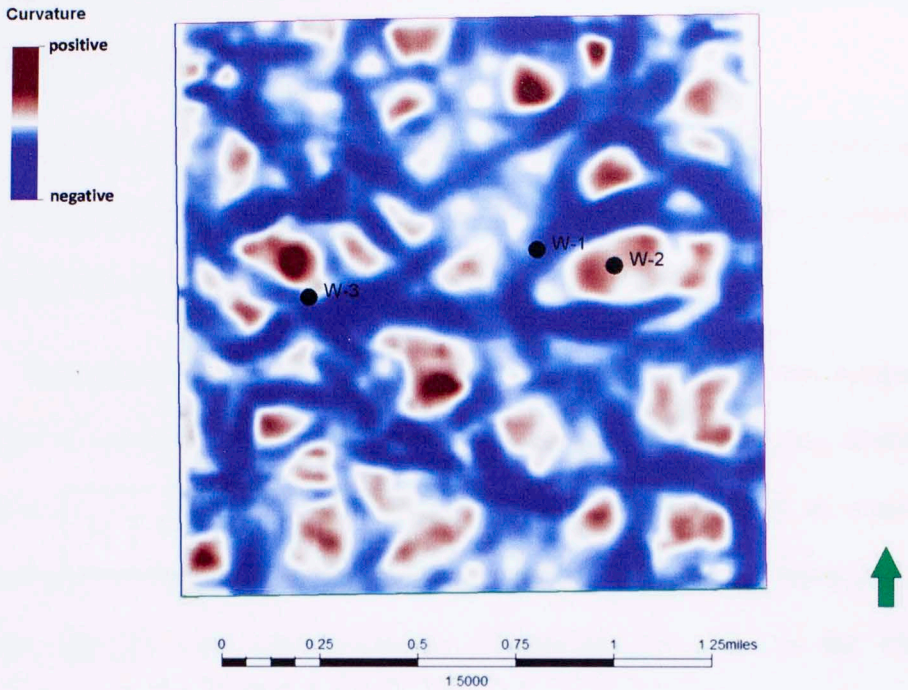

Figure 4.6 Seismic time slice through the most-negative curvature volume across the Hunton Group below the unconformity.

4.2.2 Coherence

Coherence, homogeneity or semblance is a measurement of similarity between adjacent seismic traces or waveforms that operates on a spatial fixed-length window of neighboring traces. The Sobel-filter similarity attribute is a suite of weighted-difference operators which operate at different lengths thus enhancing edges with different wavelengths (Bahorich and Farmer, 1995; Chopra and Marfurt, 2007).

Highly coherent or invariant seismic waveforms indicate high lateral continuity whereas sharp changes could indicate faulting and fracturing. Thus, interpretation and

mapping of structural and stratigraphic elements is expedited if the neighboring traces are cross-correlated in a proper spatial window.

The economic feasibility of hydrocarbons production from unconventional reservoirs is based on long-length horizontal drilling which is sometimes jeopardized by geohazards such as faults, fractures and collapse features.

Time slices through the coherence (Sobel-filter similarity) volume computed for the zone of interest reveal a continuous low coherency feature running southwest to northeast in the upper-left corner of the seismic survey as well as some other discontinuities in the middle part of the survey. The southern part is predominantly more coherent although less coherent circular features are also clear in the southwest (Figure 4.7).

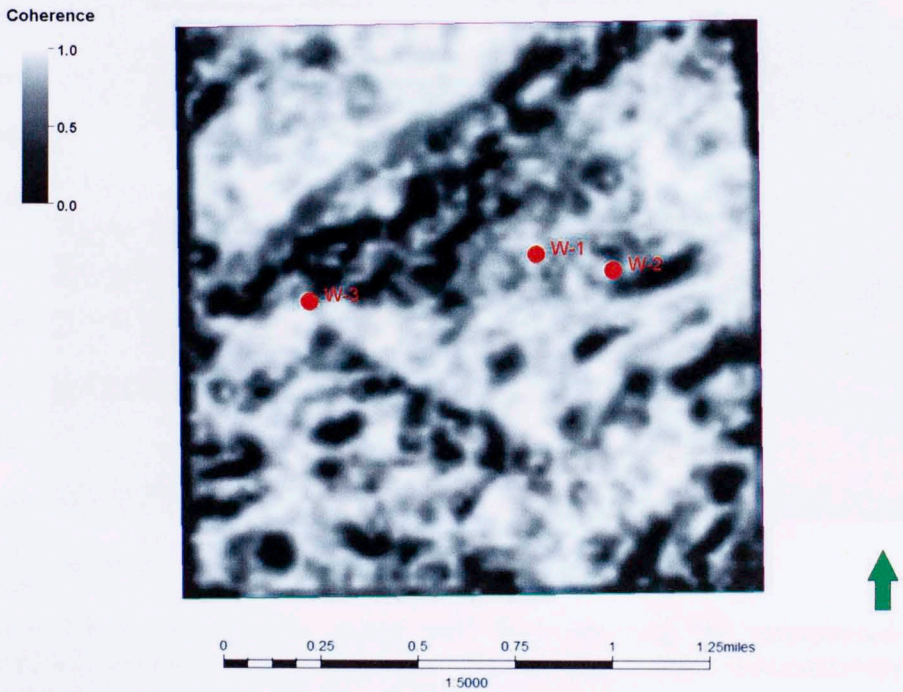

Figure 4.7 Seismic time slice through the Sobel-filter similarity volume across the Hunton Group below the unconformity showing incoherent circular and longitudinal features (black) surrounded by coherent areas (white).

4.3 SEISMIC INTERPRETATION

The reflection characters identified in the seismic-well correlations were followed and picked in the seismic survey to generate the corresponding time-structure maps for the Mayes Formation, Hunton Group and Sylvan Shale. Due to the lack of impedance contrast between the Mayes Formation and the Woodford Shale, it was not possible to continuously follow a seismic reflection correlated to this stratigraphic top (Figure 4.8). This matter will be further addressed in Section 4.4.

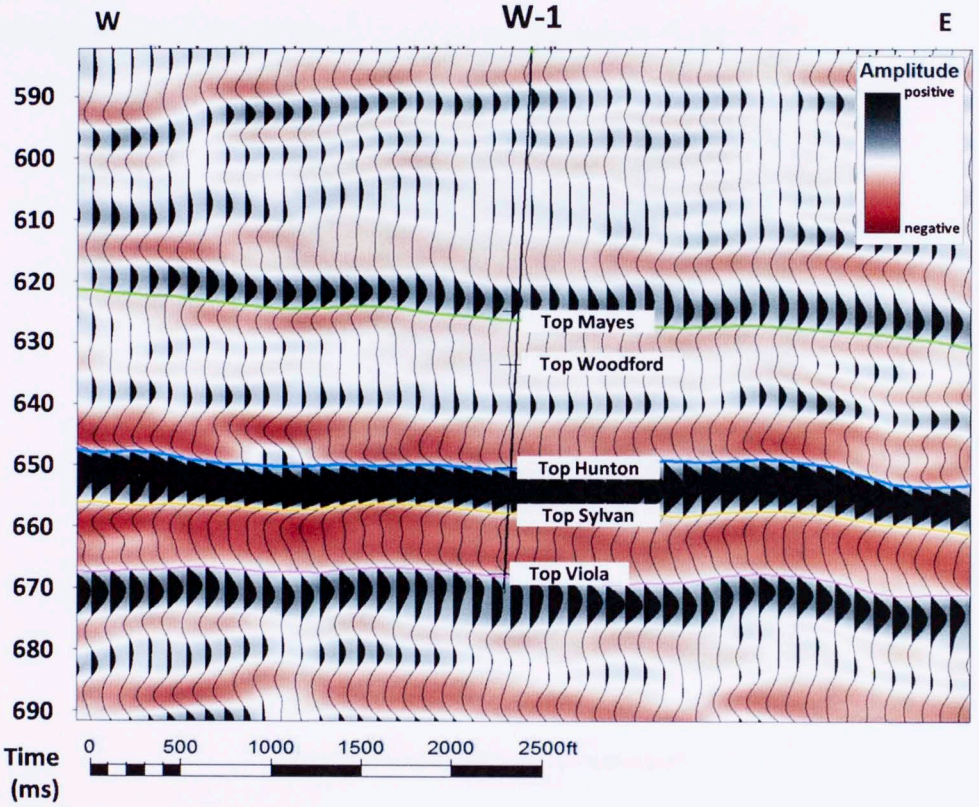

Figure 4.8 Seismic inline along well W-1 showing the interpreted Mayes, Woodford, Hunton and Viola tops. Notice the lateral discontinuity of the reflection correlated to the top of Woodford Shale.

As previously described, coherence allows to identify changes in waveform shapes whereas curvature identifies changes in dip and azimuth. When combined, they are useful tools to characterize structural elements in seismic surveys.

Several geological features were identified in the seismic data after mapping the seismic reflections correlated to the stratigraphic tops and integrating some of the observations from the seismic attributes.

A SW-NE, high angle normal fault, with a vertical separation of around 25 milliseconds, dips to the northwest and affects all of the pre-Pennsylvanian sedimentary section and probably involves the Precambrian basement (Figure 4.9).

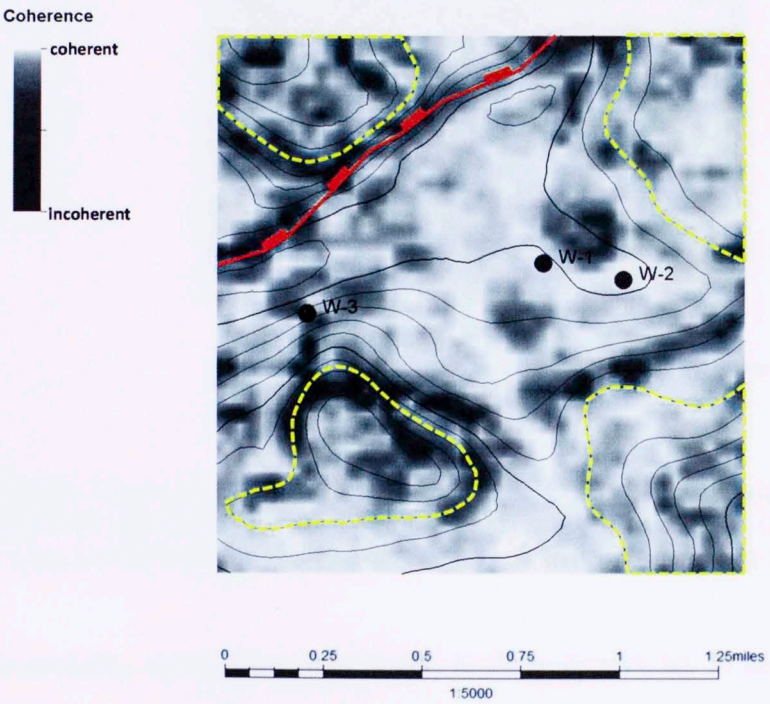

Figure 4.9 Time-structure map at the top of the Hunton Group rendered with coherence values. Notice the structural lows associated with less coherent zones (dashed yellow lines) that are interpreted as paleokarstic features.

The most-negative curvature highlights the structural lows noticed in the coherence attribute in every quadrant of the seismic survey (Figure 4.10). These features are interpreted as heavily faulted, collapsed karst-features created by the sub-aerial exposure of the Hunton Group during a major marine regression during Devonian times (Staples, 2011; Althoff, 2012)

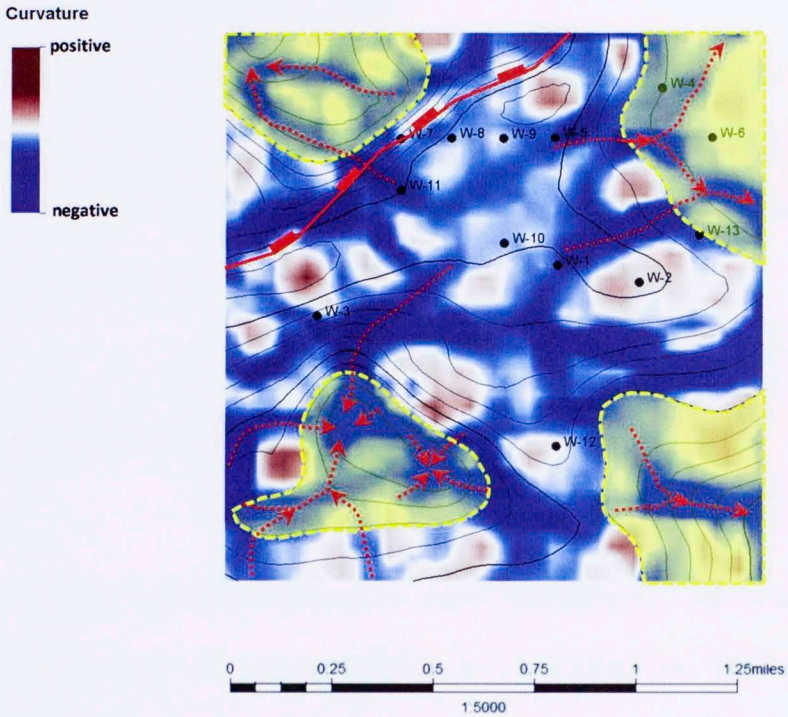

Figure 4.10 Time-structure map at the top of the Hunton Group rendered with most-negative curvature values. Notice the interpreted karsts (yellow-colored zones) associated with structural lows and negative curvatures (red arrows).

Remarkably, most of the wells drilled in the study area lay in the most-negative curvature zones at the top of the Hunton Group. Just two wells are close to most-positive curvature areas. Staples (2011), found a relationship between most-positive curvature and fracture density in the Hunton Formation and Amorocho (2012) and Gupta

(2012) relate natural fracture occurrence (from core observations and image logs) to most-positive curvature trends in the Woodford Shale. These observations have a significant impact in the prospectivity for this area as wells targeted to the Woodford and drilled through most-positive curvatures may be prone to connect natural fractures in non-karstified features. However, negative curvature on Hunton provides opportunity for thicker "sweet spots" (Slatt et al., 2014).

To further identify prospective zones based on seismic attribute interpretation, a post-stack seismic inversion was done not only to add more resolution to the seismic data but also to confidently interpret the top of the Woodford Shale in the study area and analyze its internal heterogeneities.

4.4 POST-STACK ACOUSTIC IMPEDANCE

Seismic inversion techniques allow transforming the seismic traces into impedances in order to make predictions about lithology and porosity (Russell et al., 2006). Acoustic impedance, defined as the product of density and velocity, provides one of the main advantages of the seismic inversion process over seismic amplitude data because the tuning effect is diminished and resolution is increased (Latimer et al., 2000).

Removing a wavelet from a seismic trace to obtain an appropriate reflection coefficient series yields many different solutions (Latimer et al., 2000). Different seismic inversion algorithms have been developed in order to constrain the answer and produce broadband results.

By creating a background acoustic impedance model from well data, the inverted seismic traces are modeled with the reflection coefficients obtained from the impedances at the well locations and incorporating any user-defined wavelet during the convolution process. Thus, the number of possible solutions of reflection coefficient series is constrained by the user.

Calibrated sonic logs resulting from the seismic-well tie process along with the density logs from wells W-1 and W-2 were used to build a broadband impedance model for a model-based, post-stack seismic inversion in the study area (Figure 4.11).

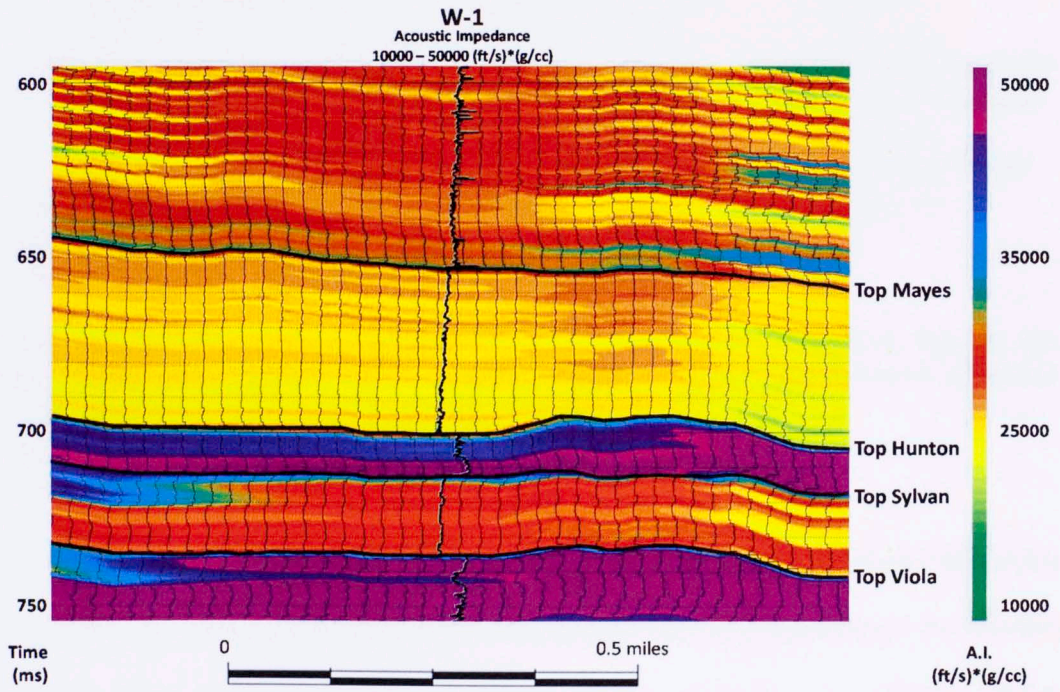

Figure 4.11 Initial broadband background model in a vertical section through well W-1 from Top Mayes to Top Viola. Inserted well log is an impedance log calculated from density and sonic logs. A high-cut frequency filter of 15 Hz was applied only to the zone of interest (Top Mayes to Top Viola).

Seismic acoustic impedances were convolved with the same wavelet extracted to create the synthetic seismograms. The resulting background model was quality-controlled by analyzing the correlation coefficients derived from the correlation of extracted composite traces along the trajectories of the boreholes and the original seismic data (Figure 4.12).

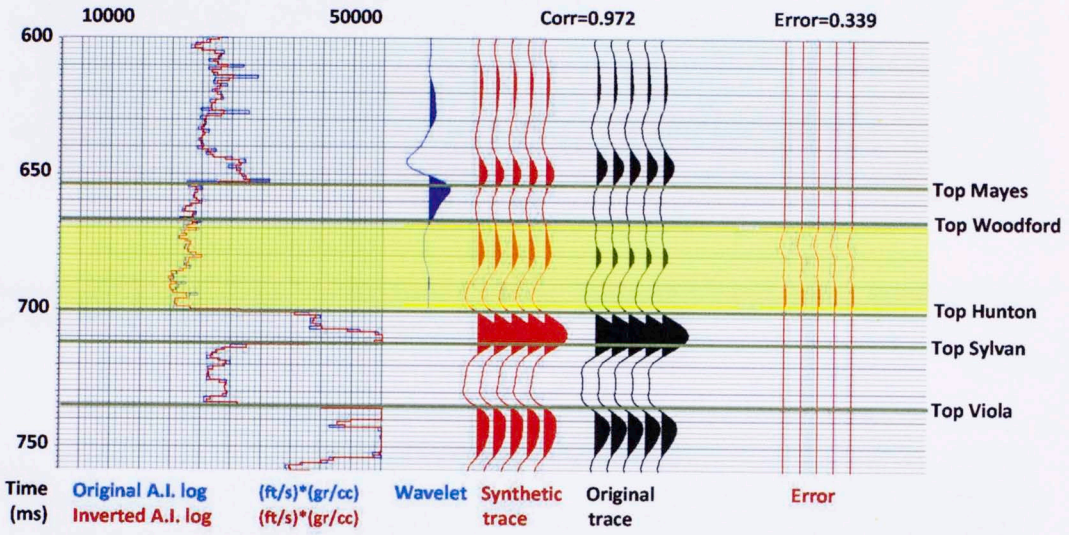

Figure 4.12 Post-stack impedance inversion analysis on well W-1. Notice the high correlation and low error obtained inside a calculation window adjusted to the Woodford Shale (yellow-shaded interval).

The acoustic impedances calculated from well logs can be cross-plotted against the impedances obtained by the seismic inversion process. High correlation coefficients and low RMS errors yield high confidence of the interactive procedure to derive impedances from seismic data (Figures 4.13 and 4.14)

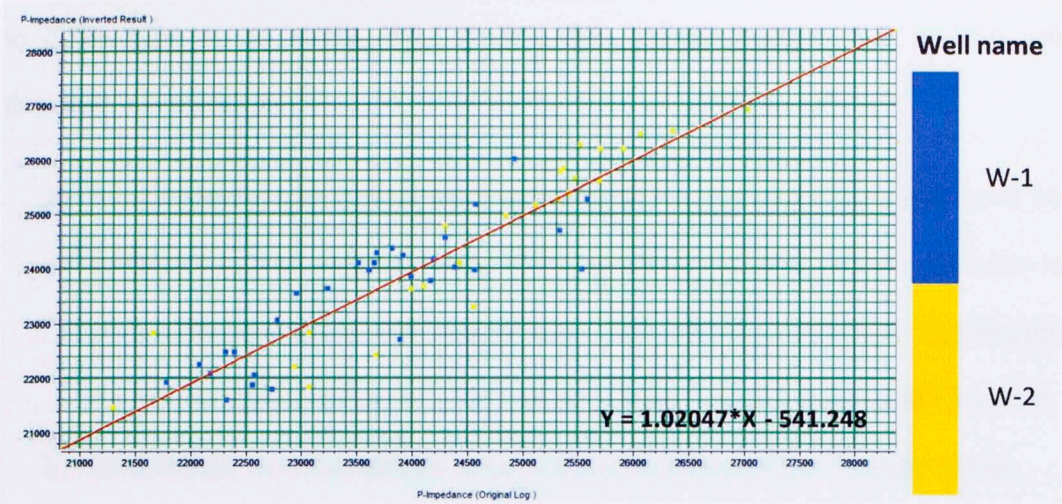

Figure 4.13 Crossplot of impedance from logs vs. Impedance from seismic inversion. Correlation coefficient: 0.917

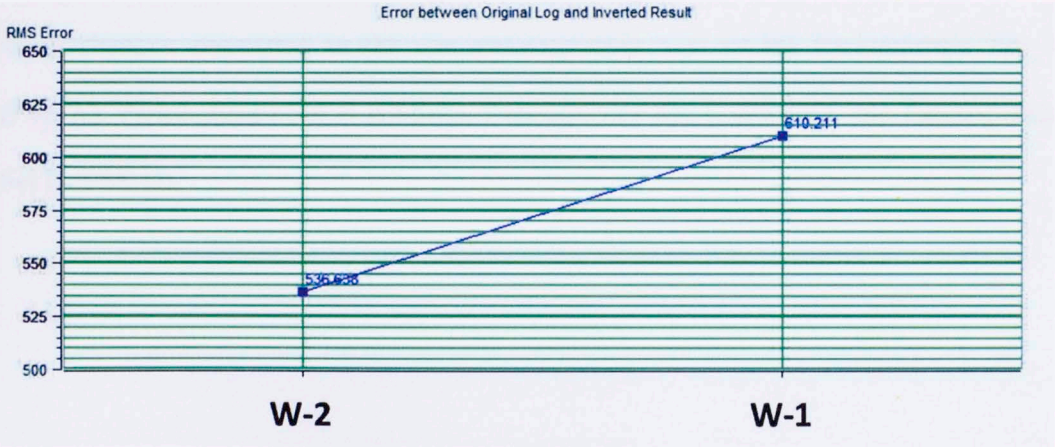

Figure 4.14 RMS prediction error between original impedance log and inverted result.

The final model-based P-impedance volume enhanced the resolution sufficiently to differentiate up to 10-feet thick strata (where enough contrast was present) and therefore was useful to:

a) Identify lateral and vertical heterogeneities in the Woodford Shale that could be correlated to total organic carbon (TOC) content and other seismic attributes to propose organic-matter rich "sweet spots" that may have economic significance for hydrocarbons exploitation. This matter will be further developed in Chapter 6.
b) Establish the lateral continuity of some of the members of the Woodford Shale.

Figure 4.15 shows an arbitrary line through well W-1. Lateral and vertical variations in impedance can be identified on the Woodford Shale. In particular, there are sharp changes associated to the chronostratigraphic tops of the Parasequence Set A (PSS-A), Parasequence Set B (PSS-B), Parasequence Set C (PSS-C), and Parasequence Set D (PSS-D).

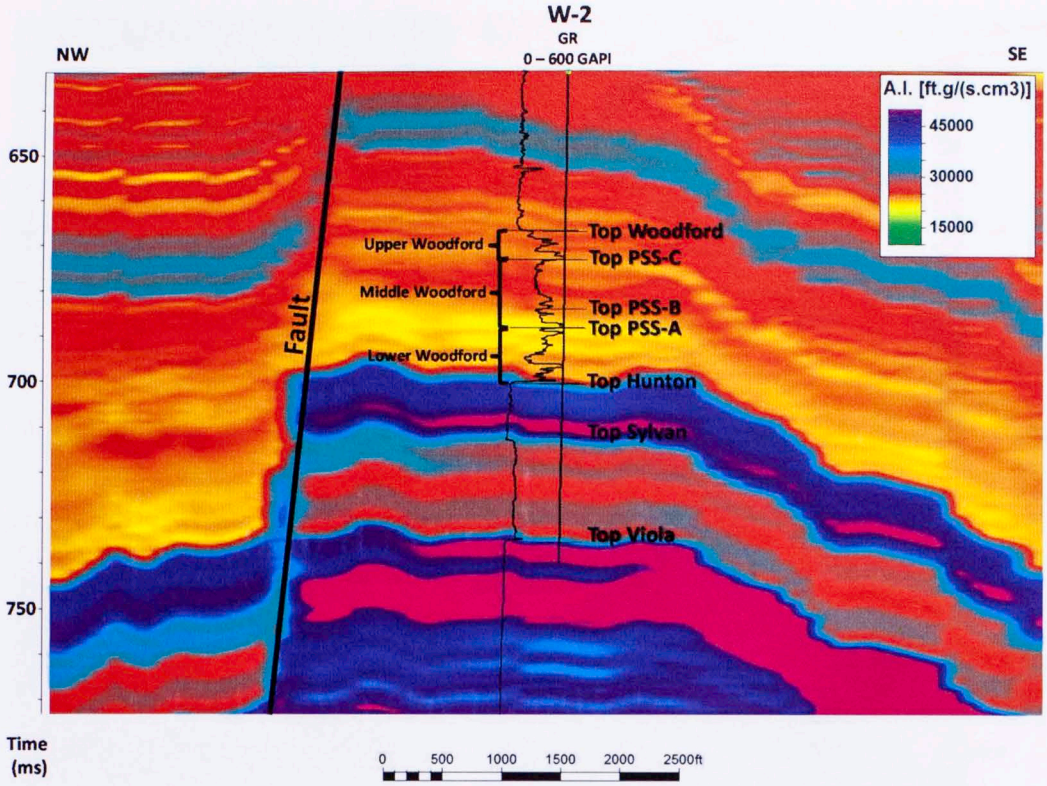

Figure 4.15 Arbitrary vertical seismic line through acoustic impedance volume showing changes in acoustic impedance inside the Woodford Shale.

These observations allowed to obtain four time-structure maps derived from impedance contrast interpretation for all Woodford Shale sequence stratigraphic units.

Figure 4.16 shows the time-structure maps at the top of all of the Woodford's parasequence sets rendered with the computed RMS impedance along this interval. Notice how impedances vary laterally due to variations in rock composition and properties.

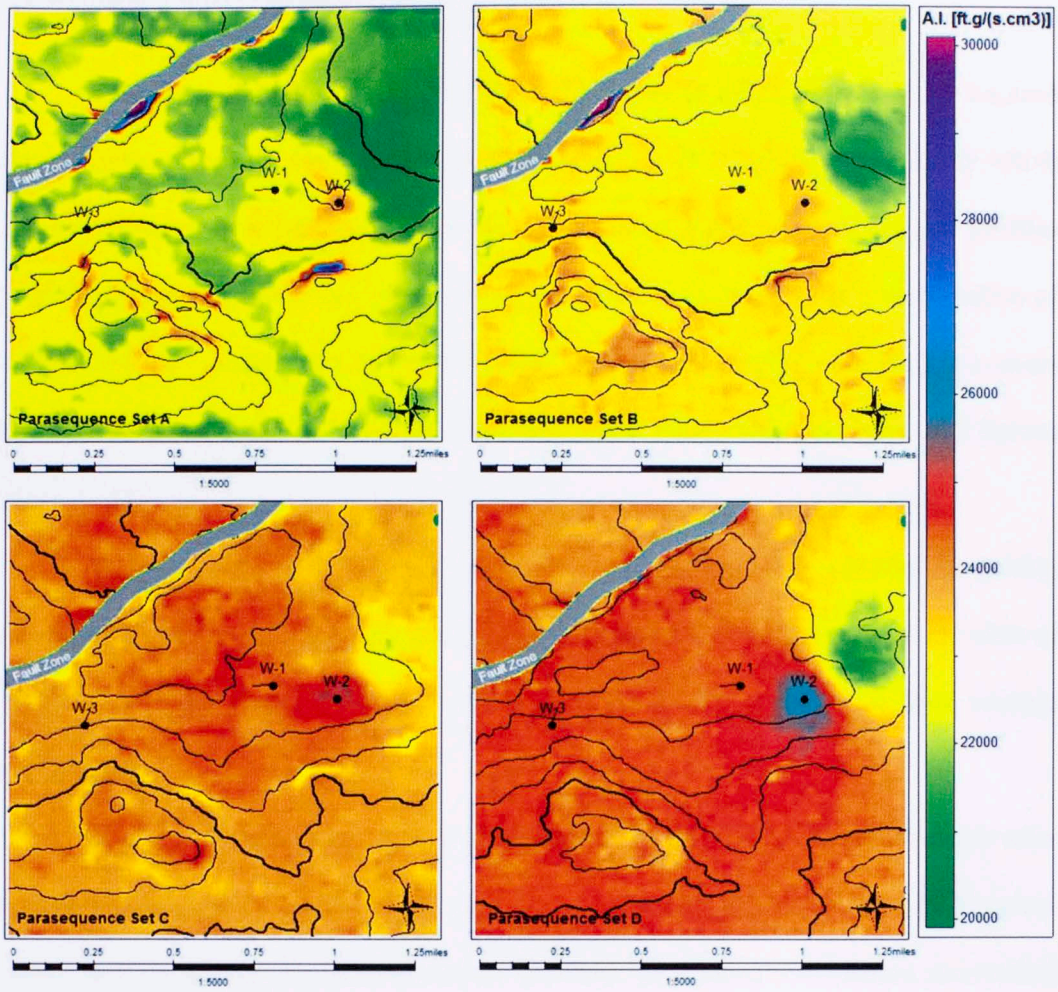

Figure 4.16 Time-structure maps at the top of the Woodford's parasequence sets, rendered with RMS impedance values.Contour interval: 10 milliseconds.

As described earlier variations in acoustic impedance may be caused by changes in rock composition and fluid content. Chapter 6 will describe how variations in impedances derived from seismic data were used to identify variations in TOC content inside the Woodford Shale.

4.5 DOMAIN CONVERSION AND THICKNESS MAPPING

Velocity is the physical quantity that relates time to depth. The velocity required for converting from the time domain to the depth domain is the P-wave velocity which can be measured in a wellbore with sonic logs, checkshots or vertical seismic profiles (VSPs), extracted from surface seismic measurements, or deduced from a combination of seismic and well measurements (Brown, 2004). This latter technique was used to convert the time-structure maps for the Top of the Woodford Shale, Hunton Group and Sylvan Shale because neither checkshots nor VSPs had been acquired in the study area.

A set of linear velocity functions (listed in Appendix B) were obtained by pairing the depth at which each stratigraphic top was interpreted in well logs with the time at which the wellbore trajectory intersects the time-structure map derived from seismic interpretation.

Figure 4.17 shows the depth-structure map at the Top of the Woodford Shale after applying the equation obtained from a series of time-depth pairs at every well location. Notice that the normal faulted anti-formal structure has a three-way closure surrounded by structural karst depressions on the Hunton Group unconformity.

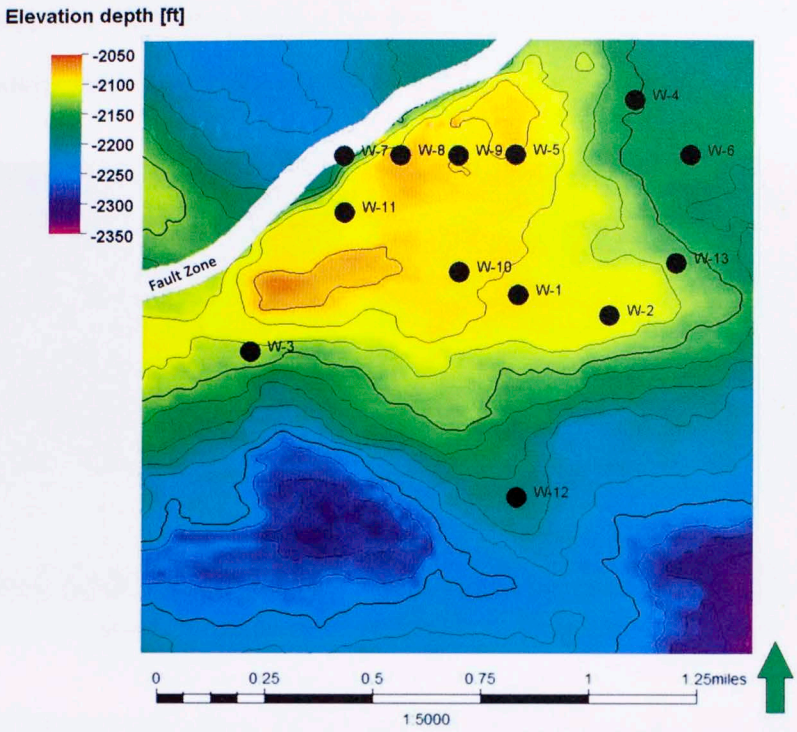

Figure 4.17 Depth-structure map at the top of the Woodford Shale.

Hunton strata are absent locally in southern Oklahoma where stream erosion was responsible for as much as 300 feet of relief during post Hunton unconformity development (Amsden, 1975; Molinares, 2013).

An isopach map of the Hunton Group (Figure 4.18a) shows the variations in thickness obtained from seismic data. A conspicuous northwest-southeast trend of low-thickness can be noticed as well as progressive thickening toward the southwestern portion of the survey suggesting the edge of an incised valley which eroded away part of the Hunton or Sylvan in this part of the Cherokee Platform to give more accommodation space to the unconformable overlying deposits of the Woodford Shale. McCullough

(2014) mapped a wider area in the Cherokee Platform and found clear evidences of the incised valleys that allowed him to describe their geometry in detail.

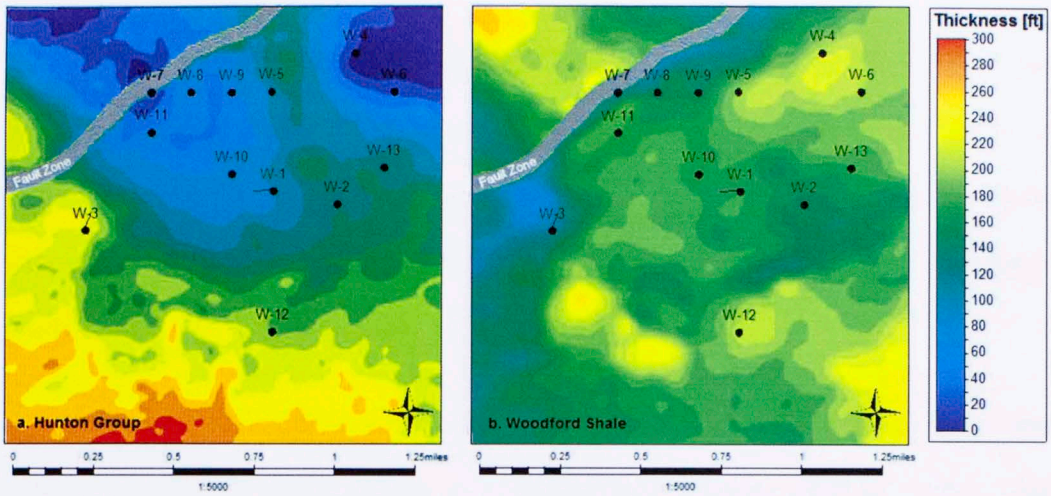

Figure 4.18 Isopach maps of (a) the Hunton Group and (b) the Woodford Shale.

The highest thicknesses of Woodford (Figure 4.18b) are associated with Hunton thins yielding to the identification of prospective spots for hydrocarbons exploration in terms not only of pay zone but also to the susceptibility to hold fractures as a consequence of karstification of the underlying Hunton limestone.

CHAPTER 5: ORGANIC GEOCHEMISTRY

Organic geochemistry identifies the influence of biological activity in the origin, evolution and distribution of chemical elements and their isotopes in the Earth. In hydrocarbon exploration and exploitation it plays a significant role in the petroleum system's evaluation by characterizing the generation, migration, and degradation processes that yield oil and gas reservoirs.

The Woodford Shale is an organic-rich source rock that is believed to have expelled around 16 billion barrels of saturated hydrocarbons (Comer, 1987). This significant petroleum-generating potential must be directly related to its volume, organic richness (quantified by total organic carbon content) and thermal maturity (quantified by the reflectance of the vitrinite maceral).

Micelli and Philp (2012) have found that in southeastern Oklahoma, the Woodford Shale has a TOC content ranging from 5.01 to 14.81% confirming its excellent hydrocarbon-generating potential. Its low maturity levels (obtained from Rock-Eval© and vitrinite reflectance analyses) forced them to conclude that it is unlikely that it has generated large quantities of hydrocarbons in this area. Nonetheless, liquid hydrocarbons have been commercially produced in some of these 'immature' areas (Smith, 2014).

5.1 SOURCE ROCK ANALYSES

In this study six drill cuttings samples from well W-2 were sent to GeoMark Research labs in order to analyze organic-richness and thermal maturity of Woodford's parasequences (Table 5.1)

PS	Depth Interval (ft)	Leco TOC (wt%)	S1 (mg HC/g)	S2 (mg HC/g)	S3 (mg HC/g)	Tmax (°C)	Calc Ro (%)	HI (S2*100/ TOC)	OI (S3*100/ TOC)
9	3070-3080	3.38	0.44	22.13	0.36	437	0.71	655	11
9	3080-3090	9.70	2.38	67.34	0.75	427	0.53	694	8
8	3090-3100	5.58	1.83	40.20	0.50	429	0.56	720	9
5	3140-3150	7.08	2.52	50.34	0.67	427	0.53	711	9
3	3170-3180	6.14	2.20	43.54	0.59	429	0.56	709	10
2	3190-3200	9.10	2.49	67.54	0.64	430	0.58	742	7

Table 5.1 Rock-Eval results from six Woodford Shale cutting samples taken from well W-2.

Rock-Eval pyrolysis analyses subject rock samples to high temperatures in the absence of oxygen, causing kerogen cracking and thus simulating thermal cooking processes in a sedimentary basin. It provides an estimate of both the amount of remaining organic-matter that can be converted into heavy hydrocarbons and the required temperature (Tmax) to achieve it. (Espitalié et al., 1985; Lafargue et al., 1998)

Vitrinite reflectance (Ro) is a tool used to assess maturity and can be calculated from Tmax values or by microscopic measurement of the amount of light reflected off of maceral fragments.

Results from Rock-Eval analyses applied to the drill cuttings reveal:

a) TOC content ranging from 3.38 to 9.7 wt% and consequently reinforcing the excellent hydrocarbon source potential of the Woodford Shale, especially in Parasequence Set A which has values above 8 wt%. Parasequence 9 in Parasequence Set D also has high values (9.7 wt%) (Figure 5.1).

b) mature enough organic-matter for liquid-hydrocarbons generation as the recorded Tmax values have a mean average of 430 °C yielding to a calculated Ro mean average of 0.58% (Figure 5.2).

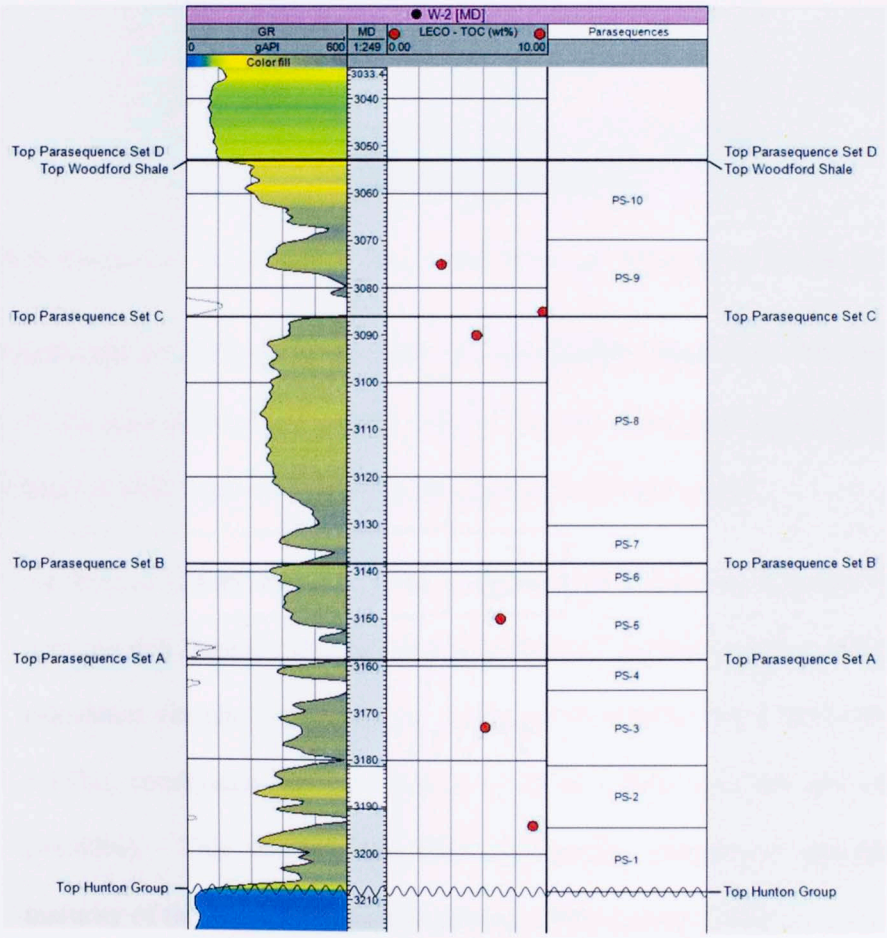

Figure 5.1 Total organic carbon content (TOC) of the Woodford Shale in well W-2.

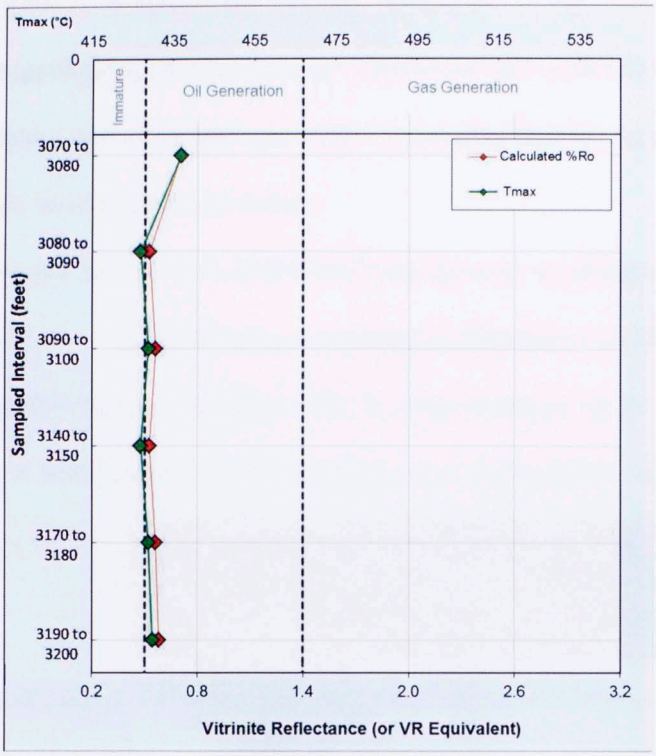

Figure 5.2 Maturity indicators (Tmax and Ro) of Woodford Shale in well W-2.

Even though the obtained Tmax values do not reach the thermal low boundary for the onset of the conventional oil window (435 °C), two facts may indicate that the Woodford Shale is able to generate liquid hydrocarbons in the study area:

a) Jarvie et al. (2005) artificially matured low maturity samples from the Type II kerogen-rich Barnett Shale redefining its thermal maturity window in terms of calculated vitrinite reflectance as: Immature (< 0.55%), oil window (0.55 to 1.15%), condensate-wet gas window (1.15 to 1.40%) and dry gas window (>1.40%). This window has been analogously adopted to describe the maturity of the Woodford Shale (Andrews, 2009; Cardott, 2012).

b) Cardott (2012) measured the vitrinite reflectance of the Woodford Shale in different geological provinces across Oklahoma and correlated them with the initial production of oil and gas wells, concluding that Ro values higher than 0.5% may be considered as mature.

c) The total gas log in well W-2 reveals an increase of methane (C1) content from 90 to more than 200 ppm, a sustained concentration of 20 ppm of ethane (C2) and the onset of propane (C3) in concentrations up to 12 ppm in the Woodford Shale interval indicating presence of hydrocarbons (Figure 5.3)

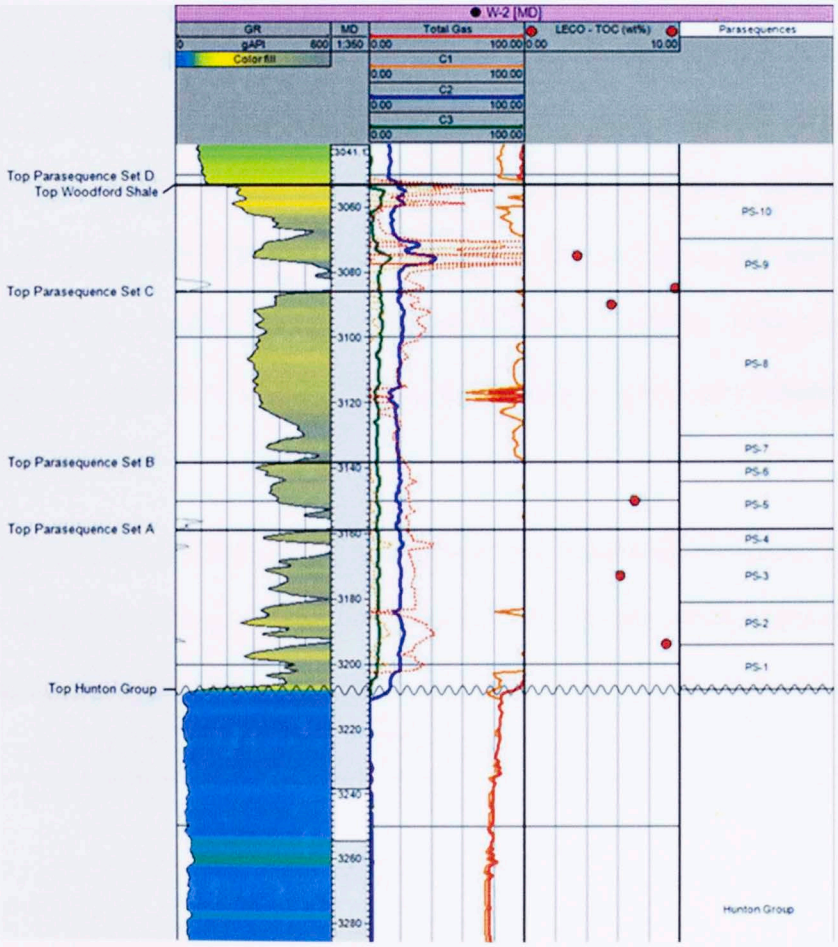

Figure 5.3 Total gas and chromatography logs (methane (C1), ethane (C2) and propane (C3)) of well W-2.

Besides Tmax, some other parameters obtained from pyrolysis analyses are considered as reliable: the hydrogen index (milligrams of hydrocarbons/grams of TOC), S1 (volume of hydrocarbons in the sample before the analysis) and S2 (volume of hydrocarbons formed during pyrolysis) values. S3 values (carbon dioxide released during kerogen cracking) provide the least reliable parameter as carbonates present in the rock may release carbon dioxide at high-temperatures (Tyson, 1995).

Part of the importance of some of these parameters is that they allow classifying the organic matter or kerogen into four types according to the ratios of hydrogen and carbon (H/C) and oxygen and carbon (O/C). The Van Krevelen diagram cross-plots these two parameters depicting both the composition of the organic matter and its gradual degradation by loss of water, carbon dioxide and hydrocarbon generation. Hydrogen (S2*100/TOC) and oxygen (S3*100/TOC) indices can be used as proxies to H/C and O/C ratios to construct pseudo Van Krevelen plots (Espitalie et al., 1977; Jarvie, 1991; Tyson, 1995), but in mature rocks they do not reveal the original kerogen quality as it changes as the organic matter degrades.

Langford and Blanc-Valleron (1990) recognized that by plotting S2 against TOC it is possible to determine the type of kerogen without using S3 data which needs to be corrected for matrix adsorption, impurities, instrumentation problems and mud additives (Peters, 1986).

Figure 5.4 shows the S2 vs TOC plot highlighting that in the study area, the preserved kerogen in the Woodford Shale has high hydrogen indices and sits at the upper limit for the Type II kerogen (HI=700 mg HC/g) proposed by Espitalié et al. (1985) and refers to organic matter with a thermal maturity corresponding to a vitrinite reflectance between 0.5 to 0.6% (Tissot and Welte, 1984).

Some of the samples plotted in this graph fall in the Type I kerogen area due to either a mixture of Type I and Type II kerogens or the presence of a hydrocarbon-rich Type I or Type II kerogens. Unfortunately, the S2 vs. TOC plot will not distinguish between these two possibilities and other information must be considered (Langford and Blac-Valleron, 1990).

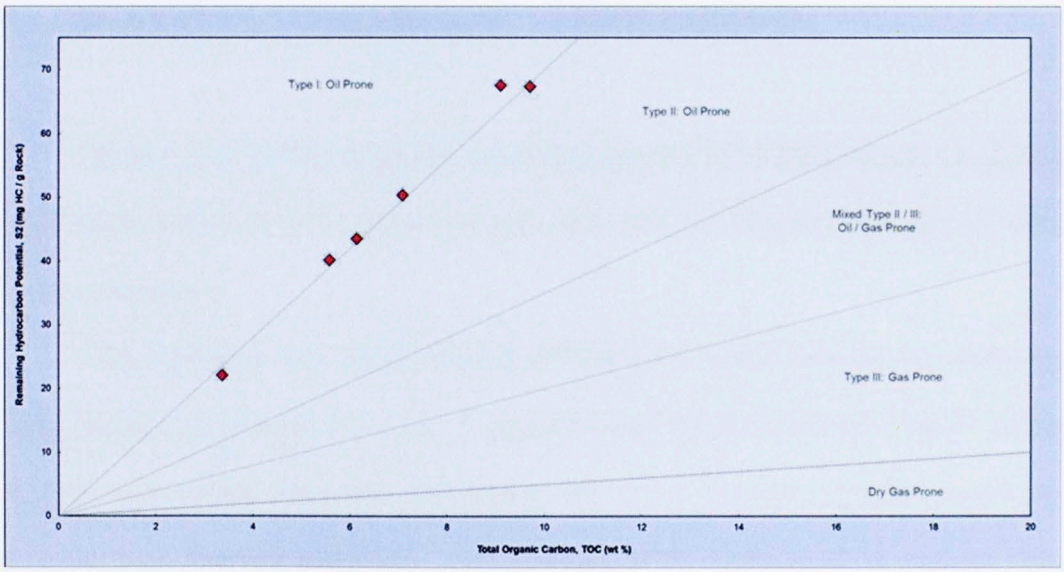

Figure 5.4 S2 vs. TOC plot illustrating the kerogen type in the Woodford Shale in the study area.

.

As stated in previous chapters, the physiographic changes in the Hunton Group exert a significant control on the depositional setting of the Woodford Shale. Some downlapping patterns have been identified in the basal member by analyzing seismic information (Slatt and Rodriguez, 2012) suggesting that some parts of the basin may have had restricted water circulation thus creating a stagnant sea with low oxygen levels and reducing conditions (Algeo et al., 2007; Molinares, 2013).

These interpretations, in conjunction with a low pollen index (PI) reported by Molinares (2013) in a well 20 miles away from the study area (Figure 2.1), indicate that the organic matter preserved in the analyzed samples contains marine Type II kerogen deposited in a stagnant basin.

5.2 LOG-DERIVED TOTAL ORGANIC CARBON CONTENT

Passey et al. (1990) developed a practical method for identifying and calculating total organic carbon (TOC) content in organic-rich rocks by using well logs, known as the *Δ log R* technique.

This technique uses the overlaying of a properly scaled porosity log (from the sonic log) on a deep resistivity curve. A separation between these curves (*Δ log R*) occurs in both hydrocarbon reservoirs and organic-rich rocks, however, at high gamma-ray intervals (non-reservoir rocks) it is a consequence of the presence of low density, low velocity kerogen whereas the resistivity curve responds to the formation fluid. The expression to calculate *Δ log R* from a sonic/resistivity overlay is:

$$\Delta \log R = \log_{10}((Res/Res_{baseline}) + 0.02 * (\Delta t - \Delta t_{baseline})).$$

(5.1)

The $\Delta \log R$ separation can then be transformed into TOC if the maturity of the organic matter (in "Level of Organic Metamorphism" units) is known by using the equation:

$$TOC = (\Delta \log R) * 10^{(2.297 - 0.1688 * LOM)}$$

(5.2)

Hood et al., (1975) introduced a depth-independent, coalification-based scale referred to as "Level of Organic Metamorphism" (LOM) to describe the progress of the thermal metamorphism of organic-matter during subsurface burial. Complementary, they related the vitrinite reflectance (Ro) as a measurement unit relative to each coalification stage from high-volatile bituminous coal to anthracite range (Figure 5.5).

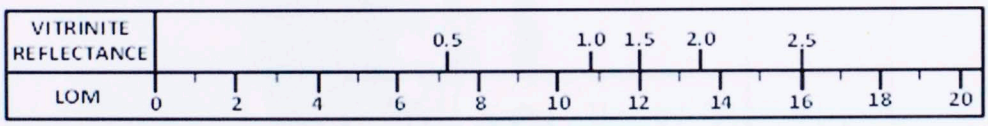

Figure 5.5 "Level of Organic Metamorphism" (LOM) scale, modified from Hood et al. (1975).

According to this scale any organic matter with a Ro higher than 0.56% but lower than 0.67% has a LOM between 8 and 9.

The results from Rock-Eval analyses performed in cuttings allowed defining a LOM of 8.7 and calibrating the calculated TOC log (Figure 5.6).

The same methodology and LOM value were used to calculate TOC logs in wells W-1 and W-3 in order to analyze vertical and lateral variations in organic matter content across the study area (Figure 5.7) and as primary input to train a neural network aiming to correlate geochemical to geophysical properties.

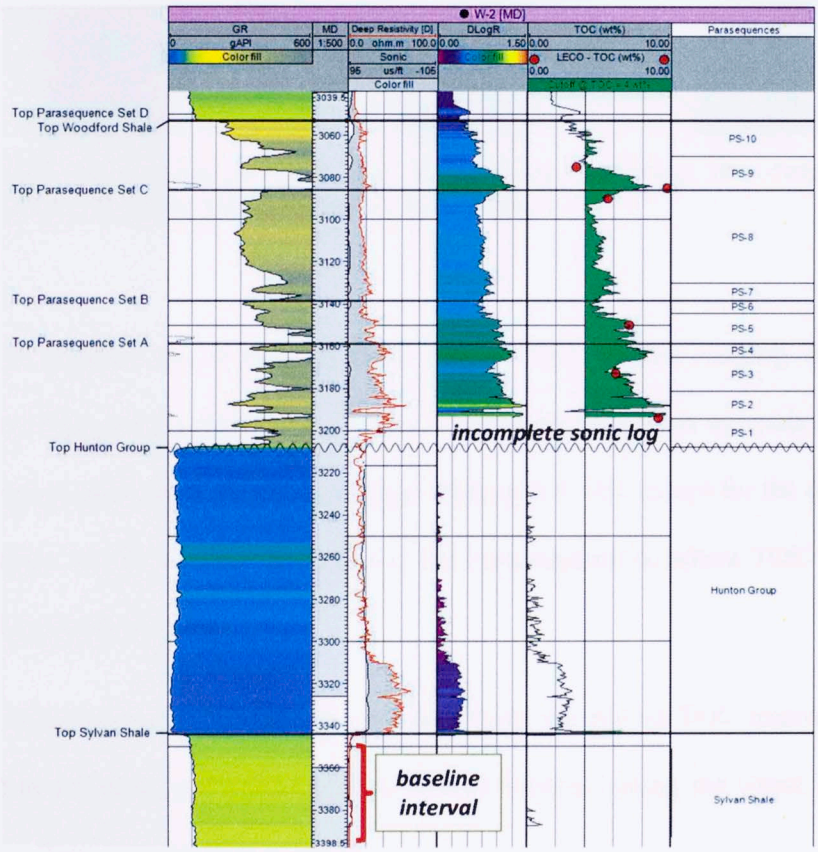

Figure 5.6 Total organic carbon (TOC) content log for well W-2 using the *Δ log R* technique. Red dots are calculated TOC values based upon Rock-Eval analyses. Fifth track from left is the calculated TOC from the *Δ log R* plot colored with a 4 wt% cutoff.

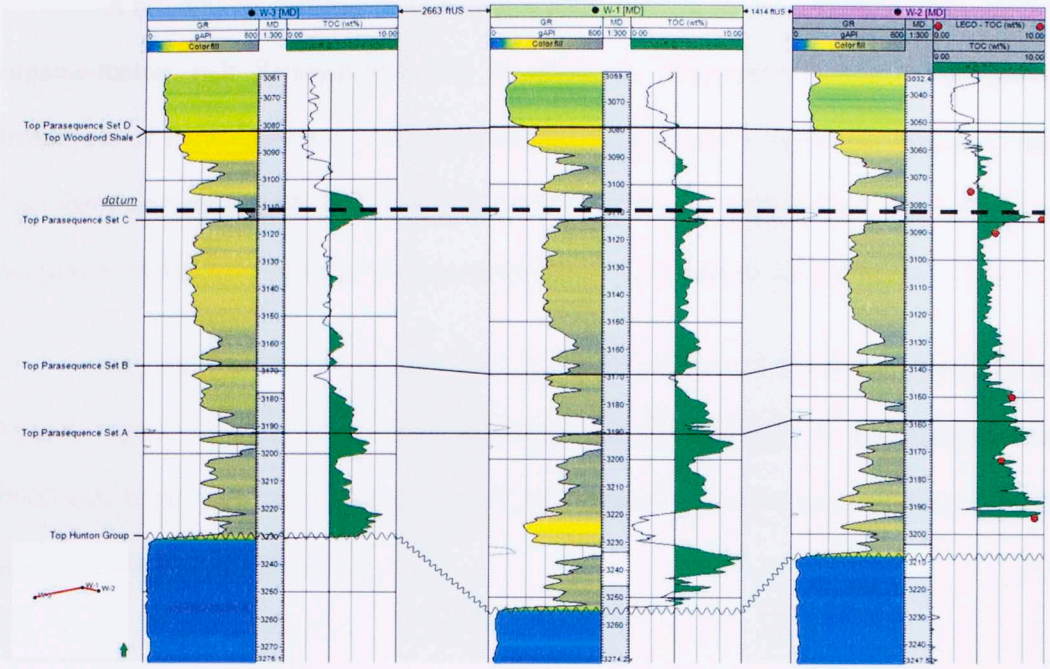

Figure 5.7 Stratigraphic well log correlation showing the total organic carbon (TOC) content distribution across wells 1-3.

In general, the Woodford Shale has a TOC content varying from 2.5 to 10.15 wt%. The strata in Parasequence Sets A and B are the richest intervals in the entire second-order sequence with a mean average value of 6.4 wt% except for the upper part of Parasequence Set B (which corresponds to the Parasequence 6) where TOC values drop to between 2.60 to 4.5 wt%.

Parasequence Set C contains comparatively the lowest TOC intervals (ranging from 3.2 to 6.2 wt%) and exhibits less vertical variation along the entire set than the underlying Parasequence Sets A and B.

A remarkable increase in TOC (up to 8.22 wt%) delineates the base of the highly organic-matter rich Parasequence Set D which is interpreted as the transgressive hemicycle of Parasequence 9 which according to Molinares (2013) corresponds to the Frasnian-Fammenian global transgression based on palynomorphs studies. The regressive hemicycle of this parasequence shows a decrease in TOC content (to 2.5 wt%).

The upper part of the Parasequence Set D (Parasequence 10) shows a cyclicity in organic-matter richness as similarly described for Parasequence 9: its transgressive hemicycle has a TOC content up to 4.7 wt% whereas its regressive hemicycle has a TOC content not higher than 3.4 wt%.

CHAPTER 6: ORGANIC-RICHNESS PREDICTION

Despite scale and resolution limitations, the integration of well and seismic data is an essential step in any effort to better characterize and map subsurface reservoir properties for hydrocarbon exploration and exploitation. In this sense, statistical algorithms play a determinant role in order to not only identify relationships (linear or non-linear) between datasets but also to quantify the level of correlation between them.

Hampson et al. (2001) introduced a combined technique of multi-attribute and neural networks analyses to determine relationships between a set of seismic attributes and reservoir properties in order to predictively compute any property throughout a seismic volume.

The simplest approach to derive a relationship between a log or property and a seismic attribute is to fit a regression line between the target log and the reference attribute. In a multivariate linear regression (used for a multi-attribute analysis) each target log sample is modeled as a linear combination of a set of attribute samples at the same time.

Such a relationship is represented by the equation:

$$L = w_0 + w_1 * A_1 + w_2 * A_2 + w_3 * A_3 + w_n * A_n, \tag{6.1}$$

where L is the target log sample, W_i is a weight applied to A_i which is the attribute sample.

The weights may be obtained by minimizing the mean-squared prediction error:

$$E^2 = \frac{1}{N}\sum_{i=1}^{N}(L_i - w_0 - w_1A_{1i} - w_2A_{2i} - w_3A_{3i} - w_nA_{ni})^2. \quad (6.2)$$

On the other hand, the best set of attributes (A_i) that better represent the desired target log (L) can be obtained by applying a *Step-wise Regression* that is not only computationally effective but also avoids picking linearly dependent attributes (Hampson et al., 2001). Later on, each selected attribute can be plotted against the target log samples (or training dataset) and a Probabilistic Neural Network (PNN) can be trained and cross-validated to calculate the best non-linear relationship between both variables, allowing a posteriori predictions (Specht, 1990; Hampson et al., 2001).

6.1 MULTI-ATTRIBUTE ANALYSIS AND NEURAL NETWORK IMPLEMENTATION

In this study, the described technique was applied in the Hampson-Russell's commercial software EMERGE©, aiming to predict total organic carbon (TOC) content using the previously calculated TOC logs along with seismic amplitudes and impedances as input variables.

The rationale for including seismic acoustic impedance as part of the analyses lay on the observation of a negative relationship, with fair correlation coefficient, between this property and TOC content (Figure 6.1) as the increase in organic-matter content negatively impacts some rock properties such as density and velocity (Passey et al., 2010; Sondergeld et al., 2010; Gupta, 2012).

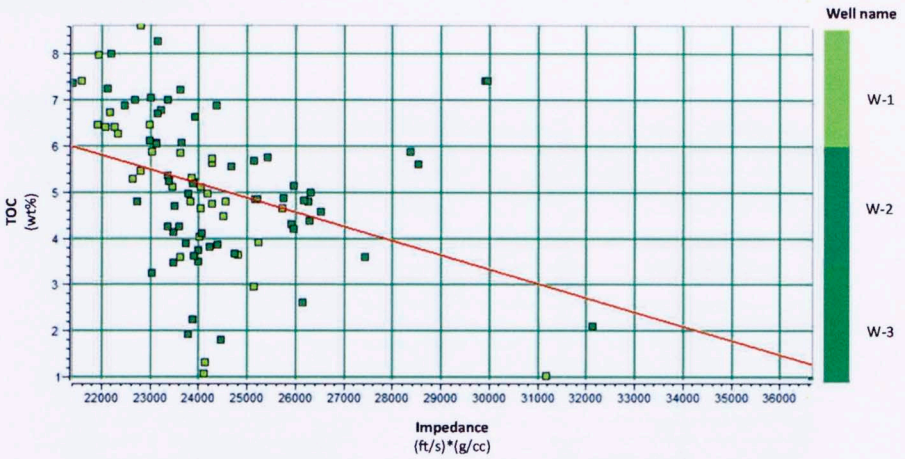

Figure 6.1 Cross-plot TOC content vs Impedance showing their negative correlation (Correlation coefficient = -0.42, slope = -0.00031, intercept = 12.63).

Various transform and EMERGE© proprietary complex trace attributes were applied to the seismic data in order to find the best set of attributes that best cross-correlates to organic-matter richness. The results of this multi-attribute analysis are shown in Table 6.1 which lists the set of attributes that are statistically significant for TOC prediction and in Figure 6.1 which illustrates their corresponding training and validation errors.

	Seismic Attribute
(1)	1 / Acoustic Impedance
(2)	(55 Hz spectral component) ^{2}
(3)	Log (60 Hz spectral component)
(4)	Seismic amplitudes
(5)	Coherent energy

Table 6.1 Computed seismic attributes and transforms for TOC content prediction by a multi-linear regression.

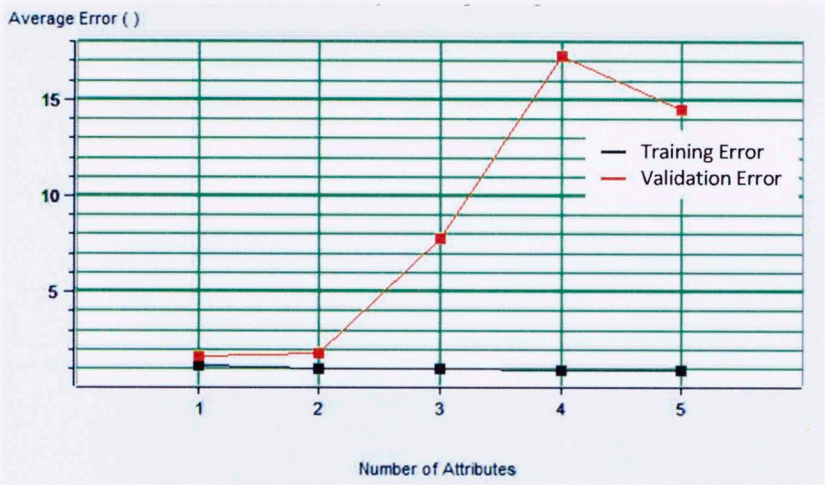

Figure 6.2 Multi-attribute training and validation errors for TOC prediction.

Based upon validation error criteria, the first two attributes have statistical significance for final TOC prediction as the average validation error after combining all of them in a multi-linear regression is around 1.3% for this specific study. If the third attribute (Log of 60 Hz spectral component) were included for TOC predictions, the validation error would increase up to 14.7%. Consequently, the first two attributes were used to create predictive pseudo-TOC logs for wells W-1 and W-2 after training and validating a Probabilistic Neural Network (PNN).

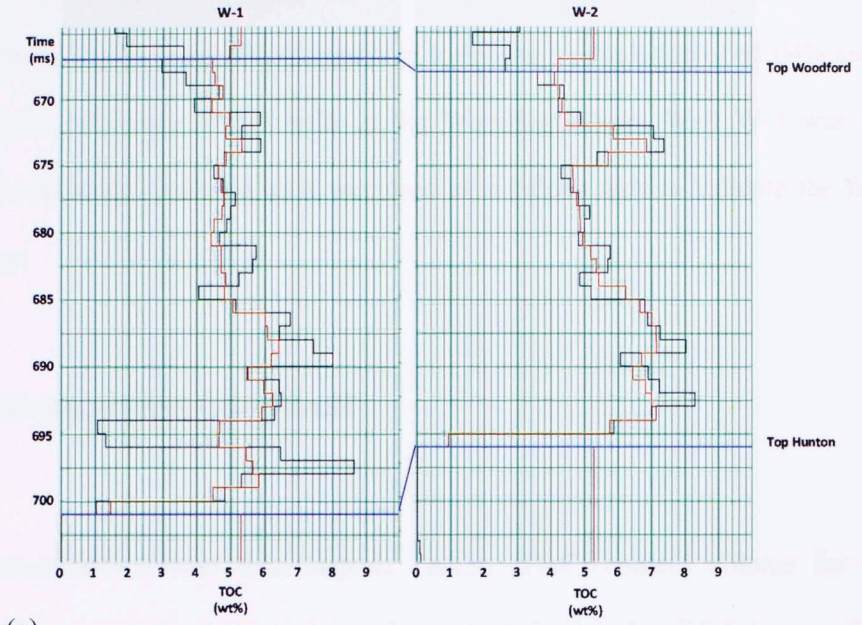

(a)

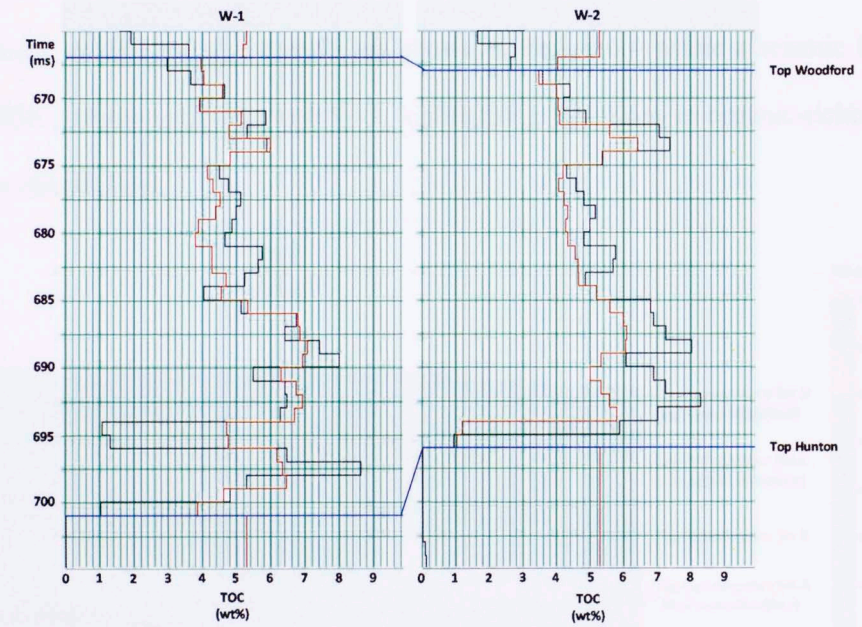

(b)

Figure 6.3 Total organic carbon (TOC) content logs used to train and cross-validate a Probabilistic Neural Network (PNN) showing (a) the training results and (b) the validation results. Black lines represent original logs and red lines represent modeled logs.

Figure 6.3 shows the training and cross-validation results obtained from the network. After validation, original and predicted logs have a correlation of 65.04% and a root-mean-square difference of 1.3 wt% in the Woodford Shale. Well W-3 was not included in the network's training as it was used as a hidden well to validate the final TOC prediction.

6.2 ORGANIC-RICHNESS CONTRAST

The seismically-derived total organic carbon (TOC) content volume for the Woodford Shale was obtained by applying the same trained and validated network to every trace in the seismic survey. Results are shown in Figure 6.4 where a seismic line through the TOC volume is tied to well W-3, highlighting variations in organic-richness across the Woodford Shale.

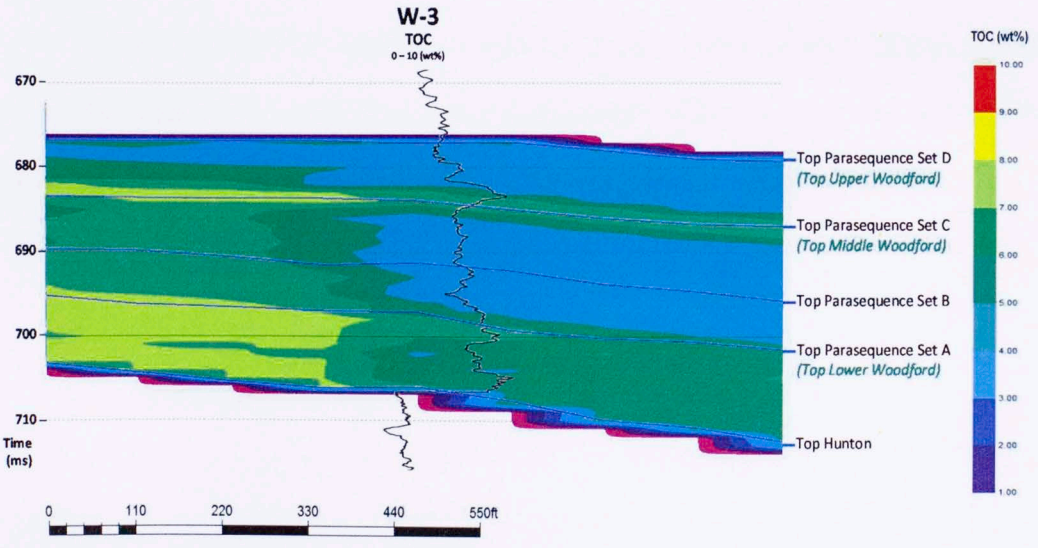

Figure 6.4 Vertical slice through the TOC content volume showing its correlation with the calculated log in the hidden well W-3.

Slatt and Rodriguez (2012) studied the sequence stratigraphy of some Paleozoic and Mesozoic shales in North America, including the Woodford Shale, and have found that these kinds of reservoirs generally are deposited upon a combined sequence boundary/transgressive surface of erosion (SB/TSE) and are a transgressive system tract (TST) enriched in organic-matter.

Aligned with these interpretations, along with observations from the previous chapter, in the study area Parasequence Sets A and B, which constitute part of the Woodford Shale's TST, are the most organic-rich intervals with TOC content ranging from 4 to 8 wt% (±1.3 wt%) whereas Parasequence Sets C and D are comparatively the poorest as their beds contain between 3 to 7 wt% (±1.3 wt%) of organic-matter.

Average TOC maps of these four parasequence sets also reveal lateral and vertical heterogeneities inside this second-order sequence that may encourage further exploratory efforts to promote prospective zones in the study area (Figure 6.5)

At first glance, the mapping reveals the same organic-matter richness pattern previously observed in vertical sections: Parasequence Sets A and B are the richest intervals whereas Parasequence Sets C and D are comparatively the poorest.

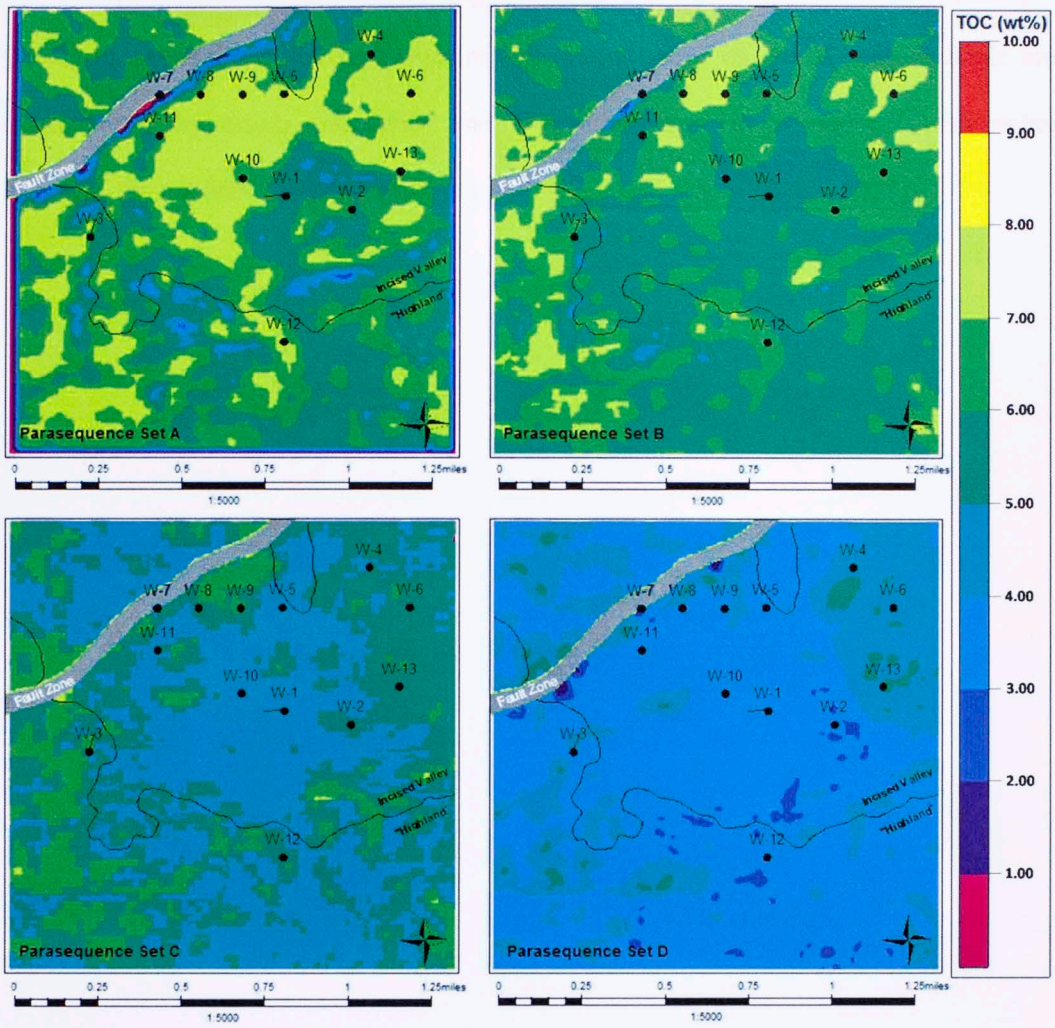

Figure 6.5 Total organic carbon (TOC) content maps for the Woodford Shale's parasequences sets in the study area. Dashed lines outline areas where this second-order sequence has more than 200 feet in thickness and are associated to pre-Woodford karsts or incised valleys.

It is also noticeable that areas associated with karstification or incised valleys, which have the thickest Woodford, do not necessarily bear intervals with the highest TOC content. Nonetheless, a certain level of TOC cyclicity can be noticed as organic-rich parasequence sets are overlain by poor ones.

This observation correlates with petrophysical interpretations done by Gupta (2012) in west-central Oklahoma where depressions filled by the Woodford Shale are characterized by cherty lithofacies and TOC-poor intervals intercalated with richer intervals, thus defining brittle-ductile couplets (Slatt and Abousleiman, 2011).

CHAPTER 7: PROSPECTIVITY

As discussed, in this area the Woodford Shale has an overall organic-richness greater than 3 wt% (±1.3 wt%) locally varying up to 8 wt% (±1.3 wt%) with a mean thickness of 178 feet as measured from structural maps in depth (Figure 7.1).

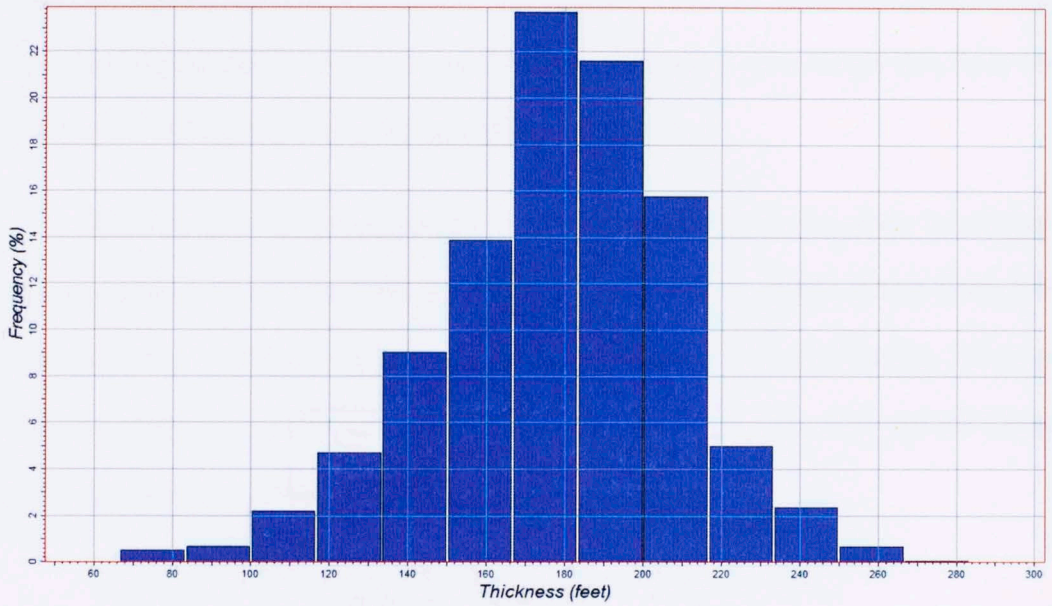

Figure 7.1 Histogram of Woodford Shale thickness in the study area.

In the exploration and exploitation of unconventional resource plays these two parameters along with kerogen quality, thermal maturity and brittle facies are determinant to maximize the well placement and hydrocarbons production. Thus, what are considered prolific shales usually contain more than 3 % TOC, are usually thicker than 200 feet, have a hydrogen index (HI) greater than 350 mg HC/g and contain kerogen Type II with a thermal maturity greater than 1.1% Ro for gas prospectivity (Slatt and Rodriguez, 2012).

Based upon thickness and organic-matter content, two prospective zones are proposed as a result of this integrated study: Prospective Zone A covers an area of 135 acres (0.46 sq-km) and is located in the central part of the study area. It has a mean thickness of 180 feet and an organic-matter richness ranging from 4 to 8 wt% (±1.3 wt%). Prospective Zone B covers an area of 125 acres (0.56 sq-km) and is located in the northeastern corner of the study area where wells W-4, W-6 and W-13 were already drilled to produce hydrocarbons from deeper reservoirs. In this zone, the Woodford Shale has an average thickness of 200 feet and its organic-matter content ranges also from 4 to 8 wt% (±1.3 wt%) across the entire sequence (Figure 7.2).

Downey et al. (2011) proposed a quantitative measure of oil-in-place for oil shale resource plays using S1 (volume of hydrocarbons in a rock sample before Rock-Eval analyses) after testing and validating their method using immature, mature and over-mature samples from cores and drill cuttings from the Eagle Ford Shale (South Texas) and in the Woodford Shale (Southern Oklahoma) (Equation 7.1).

$$OOIP\ per\ 640\frac{acre}{feet}(in\ bbl) = 9677.48 * S1_{ave},$$

(7.1)

which can be re-written as

$$OOIP\ per\ 1\ \frac{acre}{feet}(in\ bbl) = 15.12106 * S1_{ave}.$$

(7.2)

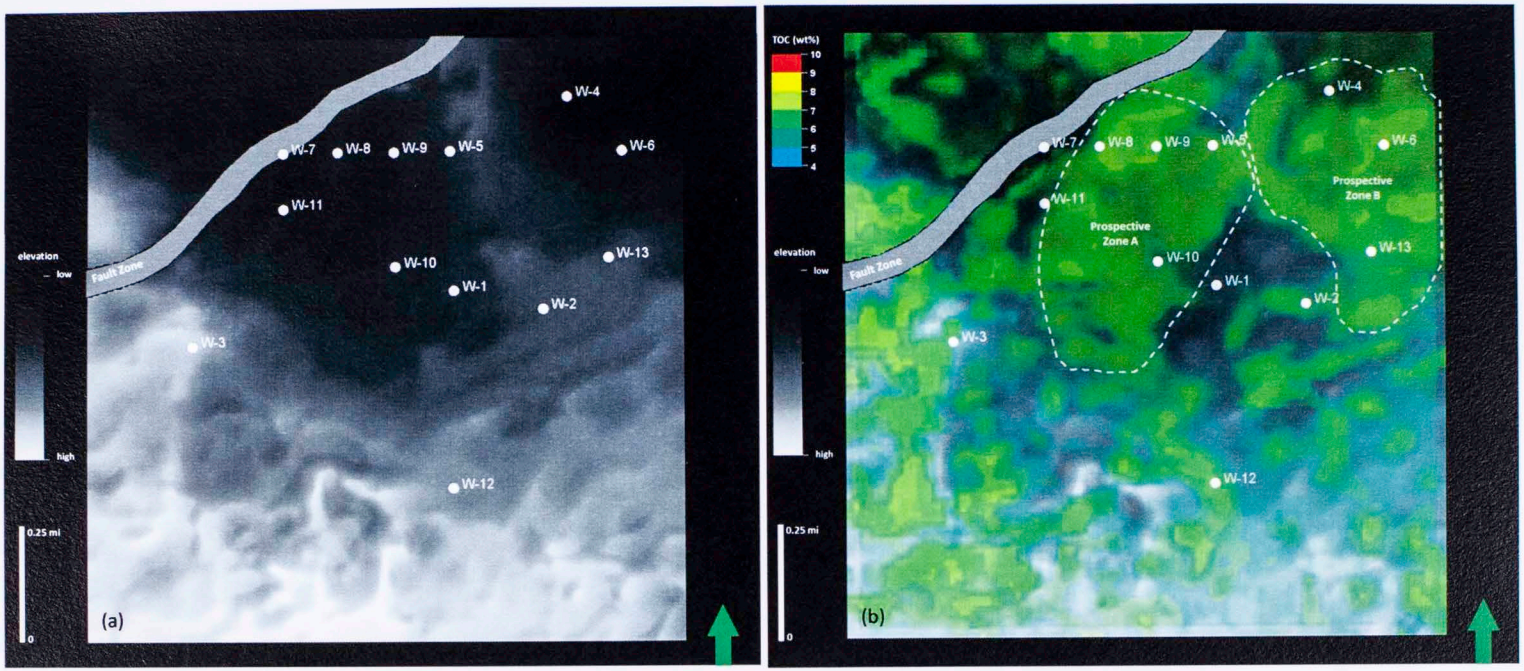

Figure 7.2 (a) Pre-Woodford pseudo-paleotopographic map of the study area and (b) total organic carbon) content average map for the Woodford Shale co-rendered with the paleotopographic map showing two prospective zones where the highest TOC content is associated with structural lows.

Rock-Eval analyses presented in Table 5.1 indicate that for the study area the Woodford Shale has an average volume of existing hydrocarbons (S1) of 1.98 mg HC/g, allowing thus to calculate an approximate potential original oil-in-place for each of the proposed prospective zones according to the areas and thicknesses noted previously (Table 7.1).

Prospective Zone	Area (acres)	Average Thickness (feet)	Average Volume (acre-feet)	OOIP (MMbbl)
A	135	180	24300	0.72
B	125	200	25000	0.74

Table 7.1 Calculated original oil-in-place for the prospective zones in the study area.

CHAPTER 8: RESULTS AND INTERPRETATIONS

The integration of multi-disciplinary data was the cornerstone to better characterize the heterogeneities of the Woodford Shale in the study area aiming to identify prospective zones or "sweet spots" based on organic-matter richness and thickness.

The qualitative and quantitative interpretation of the available seismic data allowed identifying significant physiographic changes in the basin floor caused by the Late Devonian uplift and erosion period and represented by thickness variations (from tens to hundreds of feet) of the Hunton Group. Thus, the study area sits on the edges of what is interpreted by Althoff (2012) as an incised valley that eroded away more than 200 feet of the Hunton Group where thicker Woodford Shale sediments were deposited over 33 m.a in response to eustatic sea-level changes. Furthermore, this study allowed identifying a paleo-karst/incised valley system in the southern Cherokee Platform when the Hunton was sub-aerially exposed.

Figure 8.1depicts some of the major features that can be found in karsts/valley systems due to limestone dissolution on an unconformity surface. Some of the constituents of this kind of landscape are small and steep depressions above underground caves, called *sinkholes,* which are caused by the collapse of the thinned cavern roofs (Grotzinger and Jordan, 2010).

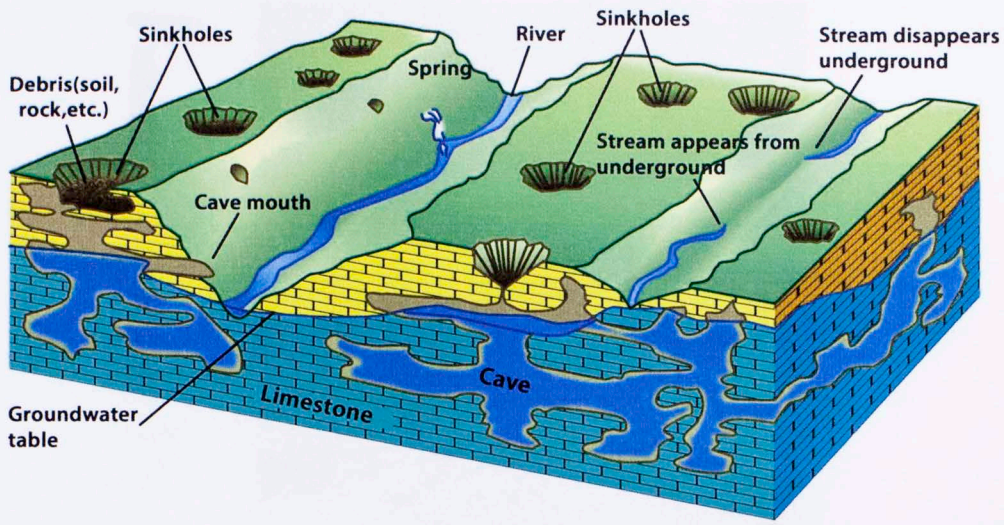

Figure 8.1 Some major features of karst topographies (Grotzinger and Jordan, 2010).

Co-rendered horizon slices taken from coherence, most-positive and most-negative seismic attributes through the top of the Hunton Group reveal some of these characteristic karst/valley-features validating the initial hypothesis that the Late Devonian drop in sea level created a dissolution landscape that latterly controlled the deposition of the Woodford Shale (Figure 8.2).

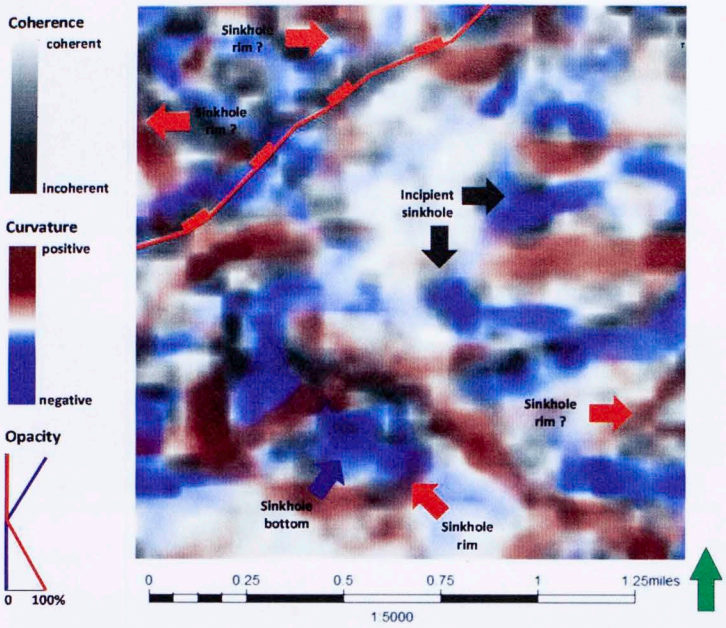

Figure 8.2 Co-rendered horizon slices of Sobel-filter similarity (coherence), most-negative and most-positive curvatures at the top of the Hunton Group.

Through a sequence stratigraphic well log interpretation, ten genetically-related higher-cyclicity deposition events or parasequences were identified in this second-order sequence which were grouped into four parasequence sets according to their distinctive aggradational, progradational or retrogradational stacking pattern.

Figure 8.3 summarizes the evolutional depositional model proposed for these four parasequence sets in the study area considering the influence the inherited karst landscape modeled by the Late Devonian regressive period that exposed sub-aerially the Hunton Group and that progressively collapsed between the Late Devonian and the Mississippian.

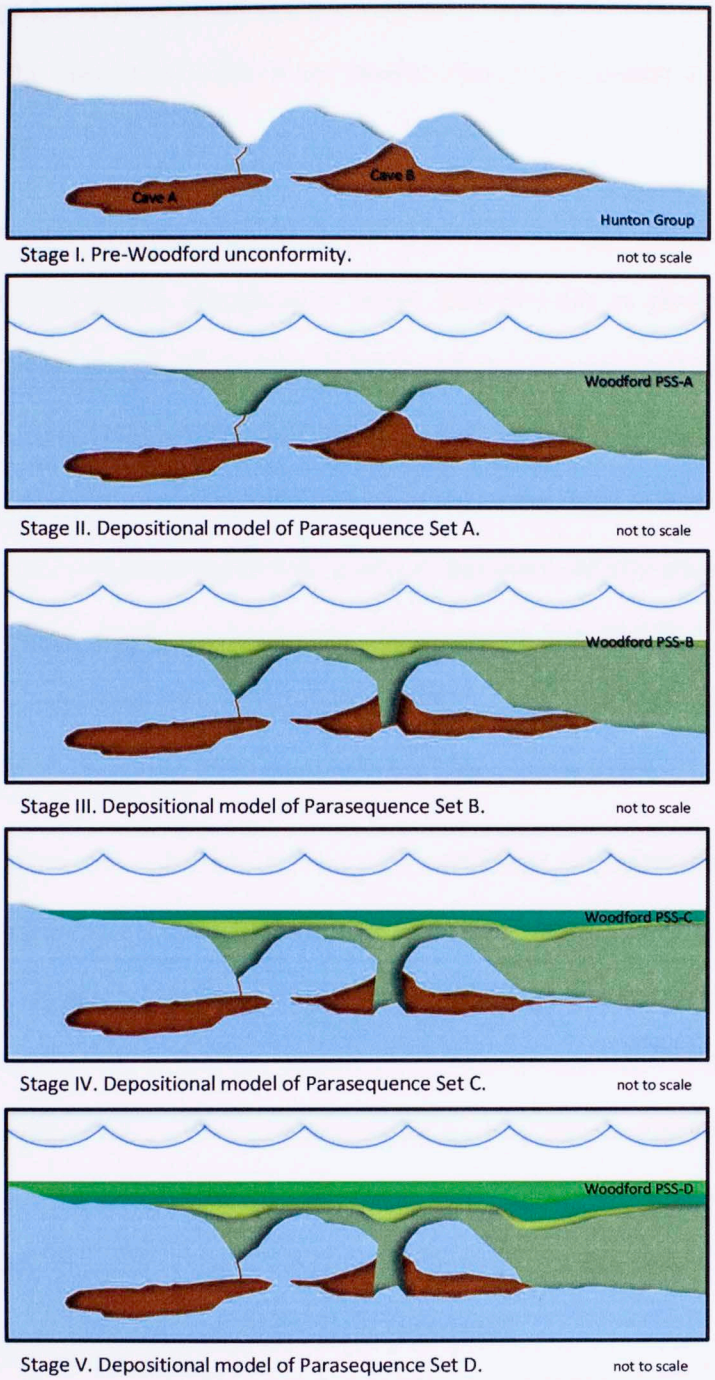

Figure 8.3 Schematic proposed depositional model of the Woodford Shale in the southern Cherokee Platform.

In Stage I, a major regional unconformity developed in the Late Devonian, eroded away part of the calcareous rocks of the Hunton Group and created a topographically irregular surface.

The Woodford's Parasequence A unconformably overlies this irregular surface after the onset of a marine transgression where karst-features as grooves, grykes and sinkholes as well as incised valleys were filled in response to a sea level rise (Stage II). In the study area, this organic-rich parasequence set is entirely equivalent to the Lower Woodford and exhibits a retrogradational pattern suggesting high accommodation space in a relatively low sediment supply with episodic deposition of less clay-rich sediments eroded from remnant Hunton pinnacles (i.e. Parasequence 2 in well W-1 in Figure 3.4). Thickness can range from 10 to 90 feet being thicker in the north and central part of the study area as more accommodation space was available (Figure 8.4a).

As transgression continues to Stage III, sediments of Parasequence Set B are conformably deposited and some underground caves of the karst system begin to collapse (caves A and B in diagram) thus creating accommodation space to hold a thicker amount of sediments. In the study area, these organic-rich strata are equivalent to the basal part of the Middle Woodford and exhibit a progradational stacking pattern suggesting a temporal reduction in the accommodation space. However, some increases in thicknesses (up to 60 feet) were locally observed in the northeastern and northwestern corners of the surveyed area in response to karst-features collapsing (Figure 8.4b).

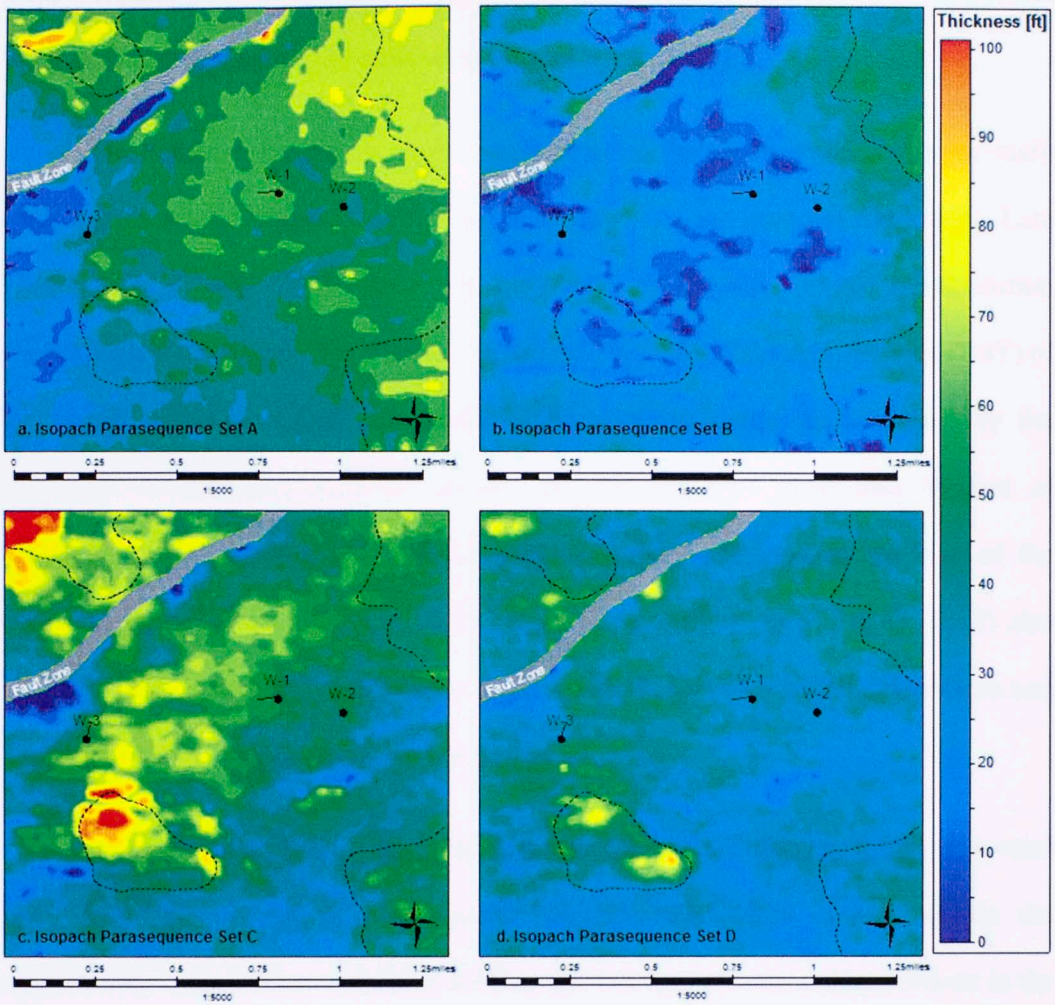

Figure 8.4 Isopach maps of (a) Parasequence Set A, (b) Parasequence Set B, (c) Parasequence Set C, and (d) Parasequence Set D illustrating the influence of karst-features collapse (outlined by dashed lines) in the preserved thickness.

Sea level continues rising during Stage IV and Parasequence Set C is conformably deposited having an aggradational-to-retrogradational stacking pattern; it is the leanest-organic interval of the entire sequence which was deposited during a sediment supply/accommodation space equilibrium period. Some karst-features collapsed, favoring

local increases of accommodation space in the southwestern and northwestern corners were up to 100 feet thick sediments were preserved (Figure 8.4c).

The Parasequence Set D, entirely equivalent to the Upper Woodford in the study area, was deposited unconformably during a major marine transgression during Late Frasnian times (Stage V) after which the sediment supply/accommodation space relation was increased, yielding to the onset of the second-order highstand systems tract (HST) of the Woodford Shale. Local increments in the accommodation space caused by the continued karst-features collapse, favored the deposition of more than 80 feet of sediments some of which are highly organic-rich especially towards the base of the parasequence set (Figure 8.4d). A similar study conducted by Baruch et al. (2012) also revealed direct influence of karst-collapse of the Ellenberger Group on the deposition and distribution of the Barnett Shale in west Texas.

A post-depositional, Late Mississippian northeast-southwest trending normal fault, that may be part of the regional Nemaha Ridge fault system, affects the northwestern corner of the study area with around 100 feet of vertical displacement in the Woodford Shale, thus creating a three-way closure anti-formal structure that has being targeted for hydrocarbons production from the Ordovician Viola Formation. However, the mature beds of the entire Woodford Shale yet may contain up to 1.46MMbls of oil-in-place in an area of approximately 260 acres thus opening a new exploratory frontier in the southern Cherokee Platform.

The entire karst system in the southern Cherokee Platform may have collapsed during Mississippian times but no conclusive evidence of this episode have been found as a consequence of this study more than the cessation of variations in thickness in the overlying Woodford's sequences as per seismic observations. Further research on this topic is required if of interest.

CHAPTER 9: CONCLUSIONS AND FUTURE WORK

The Woodford Shale in the southern Cherokee Platform is a widespread highly radioactive organic-rich source rock that was deposited unconformably during a global transgression over an irregular bottom topography caused by the uplift, erosion and karstification/valley-formation of the Silurian carbonates of the Hunton Group. In other locations, the Woodford overlies older units such as the Viola Limestone or the Sylvan Shale.

Although it has been informally subdivided into three different members (Lower, Middle and Upper) owing to particular lithological and compositional properties, its complex internal vertical and lateral heterogeneities imprinted by eustasy, sea waters circulation and biological activity require a more detailed subdivision for Woodford exploration and exploitation.

In this study, a combined reservoir characterization workflow that included geochemical, geophysical, petrophysical, sedimentological and stratigraphical analyses proved to be a valuable tool for identifying prospective zones regardless of intrinsic limitations of each particular discipline on its own.

The holistic interpretation of seismic data showed that in the study area, physiographic irregularities caused by erosion and karstification/valley formation on the Hunton unconformity surface, are directly associated to the preserved thickness of the

Woodford Shale. Thus, the sequence is commonly thicker when its underlying calcareous strata are thinner.

The proposed ten-parasequence model based on gamma ray log interpretation in conjunction with the interpretation of vertical stacking patterns may be useful in other locations not only to identify and predict genetically-related strata but also to anticipate where the most organic-rich beds may be located.

The use of acoustic inversion techniques and attributes extraction applied to the seismic data, allowed identifying, interpreting and mapping stratigraphic tops of four (may be third-order) parasequence sets that compose the Woodford Shale, thus highlithing the structural features that control its vertical and lateral preservation.

Geochemical analyses applied to drill cuttings along with well log analysis allowed to confirm not only the excellent organic-matter content (mean 6.8 ± 1.8 wt%) but also that in the study area, the Woodford Shale is in the early oil window, thus encouraging further exploratory efforts to promote its future exploitation.

The use of multi-linear regressions applied to multi-attribute analysis for seismic-based prediction of organic-richness allows identifying prospective zones or "sweet spots" in the absence of dense well control for detailed mapping, however, it is recommended to have measurements from lab analyses in order to calibrate the training data set involved in the artificial prediction.

In this sense, even though drill cuttings may bring valuable geochemical and sedimentological information, full core descriptions as well as chemical analyses done on

core samples or side-wall cores may reduce the uncertainty on the organic-richness of this heterogeneous formation.

At least thirteen wells have been drilled since the early 70s in the study area aiming to produce hydrocarbons from deeper conventional reservoirs such as the Hunton Group and Viola Formation. As some of these wells may have declined in production it would be advisable to test the rate of production of the Woodford Shale by doing a workover job. Well W-13 would be the best choice as it is located in a premium location with high gross thickness (greater than 200 feet) and high organic-matter richness (greater than 7 wt%).

REFERENCES

Algeo, T.J., T.W. Lyons, R.C. Blakey and D.J. Over, 2007, Hydrographic conditions of the Devono-Carboniferous North American Seaway inferred from sedimentary Mo-TOC relationships: Palaeogeography, Palaeoclimatology, Palaeoecology, v. 256, p. 204-230.

Al-Shaieb, Z., J. Puckette, and P. Blubaugh, 2001, The Hunton Group: sequence stratigraphy, facies, dolomitization, and karstification, in K.S. Johnson, ed., Silurian, Devonian, and Mississippian geology and petroleum in the southern Midcontinent, 1999 symposium: OGS Circular, v. 105, p. 17-29.

Althoff, C.D., 2012, Characterization of Depositional Megacycles in the Woodford Trough of Central Oklahoma: M.S. Thesis, University of Oklahoma, Norman, Oklahoma, 100 p.

Amsden, T.W., and G. Klapper, 1972, Misener Sandstone (Middle-Upper Devonian), north-central Oklahoma: AAPG Bulletin, v. 56, p. 2323-2334.

Amsden, T.W., 1975, Hunton Group (Late Ordovician, Silurian, and Early Devonian) in the Anadarko Basin of Oklahoma: OGS Bulletin, v. 121, 214 p.

Amsden, T.W., 1980, Hunton Group (Late Ordovician, Silurian, and Early Devonian) in the Arkoma Basin of Oklahoma: OGS Bulletin, v. 129, 136 p.

Amorocho, J.D., 2012, Sequence stratigraphy and seismic interpretation of the Upper Devonian-Lower Mississippian Woodford Shale in the Cherokee Platform: A characterization approach for unconventional resources: M.S. Thesis, University of Oklahoma, Norman, Oklahoma, 127 p.

Andrews, R.D., 2009, Production decline curves and payout thresholds of horizontal Woodford wells in the Arkoma Basin, Oklahoma (part 1): Shale Shaker, v. 60, p. 103-112.

Bahorich, M. and S. Farmer, 1995, 3-D seismic discontinuity for faults and stratigraphic features: The coherence cube: The Leading Edge, October 1995, 1053-1058.

Baruch, E.T., R.M. Slatt, and K.J. Marfurt, 2012, Seismic stratigraphic analysis of the Barnett Shale and Ellenburger unconformity southwest of the core area of the Newark East field, Fort Worth Basin, Texas, in J. A. Breyer, ed., Shale reservoirs—Giant resources for the 21st century: AAPG Memoir, v. 97, p. 403–418.

Blakey, R., 2014, Paleogeography and geologic evolution of North America, < http://cpgeosystems.com/nam.html>, Accessed Nov 4, 2014

Bohacs, K.M., G. J., Grawbowski, A. R., Carroll, P.J., Mankeiwitz, K.J., Miskell-Gerhardt, J.R., Schwalbach, M.B., Wegner, and J.A. Simo, 2005, Production, destruction, and dilution – the many paths to source-rock development: SEPM Special Publication, v. 82, p. 61-101.

Brown, A. R., 2004, Interpretation of three-dimensional seismic data. AAPG Memoir, v. 42. SEG Investigations in Geophysics, No. 9. 560 p.

Campbell, J.A., and R.A. Northcutt, 2001, Petroleum systems of sedimentary basins in Oklahoma, *in* Johnson K.S.; and Merriam D.F. (eds), Petroleum systems of sedimentary basins in the southern Midcontinent, 2000 symposium: OGS Circular, v. 106, p. 1-5.

Catuneanu, O., W.E. Galloway, C. Kendall, A.D. Miall, H.W. Posamentier, A. Strasser, and,M.E. Tucker, 2011, Sequence stratigraphy: Methodology and Nomenclature. Newsletters on Stratigraphy, v. 44/3, p. 173-245.

Cardott, B.J., and M.W. Lambert, 1985, Thermal maturation by vitrinite reflectance of Woodford Shale, Anadarko basin, Oklahoma: AAPG Bulletin, v. 69, p. 1982-1998.

Cardott, B. J., 2012, Thermal maturity of Woodford Shale gas and oil plays, Oklahoma, USA: International Journal of Coal Geology, v. 103, p. 109–119.

Cardott, B.J., 2013, Woodford Shale: From hydrocarbon source rock to reservoir. Search and Discovery Article #50817. 85 slides.

Chopra, S., and K.J. Marfurt, 2007, Seismic attributes for prospect identification and reservoir characterization: SEG Geophysical Developments Series, No 11, 464 p.

Comer, J. B., 1987, Recognizing and quantifying expulsion of oil from the Woodford Formation and age-equivalent rocks in Oklahoma and Arkansas: AAPG Bulletin, v. 71, p. 844-858.

Comer, J. B., 1991, Stratigraphic analysis of the Upper Devonian Woodford Formation, Permian Basin, West Texas and Southeastern New Mexico: Texas Bureau of Economic Geology Report of Investigations, v. 201, 63 p.

Comer, J. B., 2007, Lithologic characteristics and gas production potential of Woodford Shale in the southern Midcontinent: 2007 Geological Society of America Annual Meeting and Exposition – Abstracts with programs, p. 356.

Comer, J.B., 2008, Reservoir characteristics and production potential of the Woodford Shale: WorldOil Magazine, v. 229, No. 8.

Downey, M.W., J. Garvin, R.C. Lagomarsino, and D.F. Nicklin, 2011, Quick-look determination of oil-in-place in oil shale resource plays: Search and Discovery Article #40764.

Espitalié , J., G. Deroo, and F. Marquis, 1985, La pyrolyse Rock-Eval et ses applications. 1ere partie: Revue de l'Institut Francais du Petrole, v. 40, p. 563–579.

Friess, J.P., 2005, The southern terminus of the Nemaha Tectonic Zone, Garvin County, Oklahoma: Shale Shaker, September-October 2005, p. 1-13.

Grotzinger, J.G and T.H Jordan, 2010, Understanding Earth. W. H. Freeman; Sixth Edition, 672 p.

Gupta, N., 2012, Integrated characterization of the Woodford Shale in Westcentral Oklahoma: Ph.D. Dissertation, University of Oklahoma, Norman, Oklahoma, 156 p.

Hampson, D., J.S. Schuelke, and J.A. Quirein, 2001, Use of multi-attribute transforms to predict log properties from seismic data: Geophysics, v. 66, p. 220-236.

Hemmesch, N. T., et al 2014. A sequence-stratigraphic framework for the Upper Devonian Woodford Shale, Permian Basin, west Texas: AAPG Bulletin, v. 98, No. 1, p. 23-47.

Henry, M.E. and Hester, T.C., Anadarko basin province (058). http://certmapper.cr.usgs.gov/data/noga95/prov58/text/prov58.pdf, Accessed Nov 04, 2014.

Hood, A., C.M. Gutjahr, and R.L. Heacock, 1975, Organic metamorphism and the generation of petroleum: AAPG Bulletin, v. 59, p. 986-996.

Houseknecht, D.W., W.A. Rouse, S.T. Paxton, J.C. Mars, and B. Fulk, 2014, Upper Devonian–Mississippian stratigraphic framework of the Arkoma Basin and distribution of potential source-rock facies in the Woodford–Chattanooga and Fayetteville–Caney shale-gas systems: AAPG Bulletin, v. 98, p. 1739-1759.

Jarvie, D.M., 1991, Total organic carbon (TOC) analysis. Chapter 11: Geochemical methods and exploration: AAPG Treatise of petroleum geology: Source and Migration Processes and Evaluation Techniques, p. 113-118.

Jarvie, D.M., R.J. Hill, and R.M. Pollastro, 2005, Assessment of the gas potential and yields from shales: The Barnett Shale Model. In: Cardott, B.J. (Ed.), Unconventional Energy Resources in the Southern Midcontinent, 2004 Symposium: Oklahoma Geological Survey Circular, v. 110, p. 37–50.

Johnson, K.S., 2008, Geologic history of Oklahoma: OGS Educational publication, v. 9, 6 p.

Killian, B.J., 2012, Sequence stratigraphy of the Woodford Shale, Anadarko Basin, Oklahoma: Implications on regional Woodford target correlation: M.S. Thesis, University of Oklahoma, Norman, Oklahoma, 127 p.

Kirkland, D.W., R.E. Denison, D.M. Summers, and J.R. Gormly, 1992, Geology and organic geochemistry of the Woodford Shale in the Criner Hills and western Arbuckle Mountains, Oklahoma, *in* K. S. Johnson and B. J. Cardott, eds., Source rocks in the southern mid-continent: 1990 Symposium: OGS Circular, v. 93, p. 38–69.

Klein, P., L. Richard, and H. James, 2008, 3D curvature attributes: a new approach for seismic interpretation: First Break, v. 26, p. 105-112.

Kuykendall, M.D., and Fritz, R.D., 2001, Misener Sandstone of Oklahoma. AAPG Search and Discovery Article #10018, 74 p.

Lafargue, E., F. Marquis, and D. Pillot, 1998, Rock-Eval 6 applications in hydrocarbon exploration, production, and soil contamination studies: Revue de l'Institut Francais du Petrole, v. 53, p. 421–437.

Lambert, M.W., 1992, Internal stratigraphy of the Chattanooga Shale in Kansas and Oklahoma, in K.S. Johnson and B.J. Cardott, eds., Source rocks in the southern Midcontinent, 1990 symposium: OGS Circular, v. 93, p. 94-105.

Langford, F.F. and M.M. Blanc-Valleron, 1990, Interpreting Rock-Eval pyrolysis data using graphs of pyrolizable hydrocarbons vs. total organic carbon: AAPG Bulletin, v. 74, p. 799-804.

Latimer, R.B., R. Davidson, and P. Van Riel, 2000, An interpreter's guide to understanding and working with seismic -derived acoustic impedance data: The Leading Edge, v. 19, p. 242–256.

McCullough, B.J., 2014, Sequence stratigraphic framework and characterization of the Woodford Shale within major incised valley fill depositional patterns of the southern Cherokee Platform of south-central Oklahoma, M.S. Thesis, University of Oklahoma, Norman, Oklahoma, in press.

Miceli, A.A., and R.P. Philp, 2012, Organic geochemistry of the Woodford Shale, southwestern Oklahoma: How variable can shales be?: AAPG Bulletin, v. 96, No. 3, p. 493-517.

Mitchum, R.M., JR., 1977, Glossary of terms used in seismic stratigraphy: Seismic Stratigraphy – Applications to Hydrocarbon Exploration, AAPG Memoir, v. 26, p. 205-212.

Molinares, C.E., 2013, Stratigraphy and palynomorphs composition of the Woodford Shale in the Wyche Farm shale pit, Pontotoc County, Oklahoma. M.S. Thesis, University of Oklahoma, Norman, Oklahoma, 90 p.

Northcutt, R.A., K.S. Johnson, and G.C. Hinshaw, 2001, Geology and petroleum reservoirs in Silurian, Devonian, and Mississippian rocks in Oklahoma, in K.S. Johnson, ed., Silurian, Devonian, and Mississippian geology and petroleum in the southern Midcontinent, 1999 symposium: OGS Circular, v. 105, p. 1-15.

Passey, Q.R., S. Creaney, J.B. Kulla, F.J. Moretti, and J.D. Stroud, 1990, A practical model for organic richness from porosity and resistivity logs: AAPG Bulletin, v.74, p.1777-1794.

Passey, Q. R., K.M., Bohacs, R. Esch, and S. Sinha, 2010, From oil-prone source rock to gas-producing shale reservoir – Geologic and petrophysical characterization of unconventional shale gas reservoirs, Paper SPE 131350

Paxton, S.T., A.M. Cruse, and A.M. Krystyniak, 2006, Fingerprints of global sea-level change revealed in Upper Devonian/Lower Mississippian Woodford Shale of south-central Oklahoma. AAPG Search and Discovery Article #4021. 47 slides.

Peters, K.E., 1986, Guidelines for evaluating petroleum source rock using programmed pyrolysis: AAPG Bulletin, v.70, p. 318-329.

Portas, R.M., 2009, Characterization and origin of fracture patterns in the Woodford Shale in southeastern Oklahoma for application to exploration and development, M.S. Thesis, University of Oklahoma, Norman, Oklahoma, 110 p.

Posamentier, H.W. and D.P. James, 1993, An overview of sequence-stratigraphic concepts: Uses and abuses. Spec. Publs Int. Ass. Sediment, v. 18, p. 3-18.

Posamentier, H.W., and G.P. Allen, 1999, Siliciclastic sequence stratigraphy. Concepts and applications, Concepts in Sedimentology and Paleontology: SEPM, v. 7, 210 p.

Roberts, A., 2001, Curvature attributes and their applications to 3D interpreted horizons: First Break, v. 19, p. 85-99.

Russell, B., D. Hampson, and B. Bankhead, 2006, An inversion primer: CSEG Recorder, v. 31, No. 10, p. 101-108.

Serna, A., 2013, Geological characterization of the Woodford Shale, McAlister Cemetery Quarry, Criner Hills, Ardmore Basin, Oklahoma: M.S. Thesis, University of Oklahoma, Norman, Oklahoma, 141 p.

Slatt, R.M., and Y. Abousleiman, 2011, Merging sequence stratigraphy and geomechanics for unconventional gas shales: The Leading Edge, v.30, p. 274-282.

Slatt, R.M., and N.D. Rodriguez, 2012, Comparative sequence stratigraphy and organic geochemistry of gas shales: Commonality or coincidence. Journal of Natural Gas Science and Engineering, v. 8, p. 68-84.

Slatt, R., 2013, Sequence stratigraphy of the Woodford Shale and application to drilling and production. Search and Discovery #50792, 20 p.

Slatt, R.M., C. Molinares-Blanco, J.D. Amorocho, C.L. Cabarcas and E. Torres-Parada, 2014, Sequence stratigraphy, geomechanics, microseismicity, and geochemistry relationships in unconventional resource shales, Paper URTeC #1934195

Smith, P.W., 2014, Early identification of and oil play in the Woodford Shale in Central Oklahoma: Process and Results. Oral presentation. Woodford Oil Congress 2014.

Sondergeld, C.H., K.E. Newsham, J.T. Comisky, M.C. Rice, and C.S. Rai, 2010, Petrophysical considerations in evaluating and producing shale gas resources: SPE Unconventional Gas Conference, Pittsburg, Pennsylvania, USA, Society of Petroleum Engineers. Paper SPE 131768.

Specht, D., 1990, Probabilistic neural networks: Neural Networks, v. 3, p. 109–118.

Staples, E.R., 2011, Subsurface and experimental analyses of fractures and curvature, M.S. Thesis, University of Oklahoma, Norman, Oklahoma, 88 p.

Sullivan, K.L., 1985, Organic facies variation of the Woodford Shale in western Oklahoma: Shale Shaker, v. 35, p. 76-89.

Tissot, B.P., and D.H. Welte, 1984, Petrolewum formation and occurrence, Second Edition: Berlin, Springer-Verlag, 699p.

Treanton J., 2014, Outcrop-derived chemostratigraphy of the Woodford Shale, Murray County, Oklahoma: M.S. Thesis, University of Oklahoma, Norman, Oklahoma, 83 p.

Tyson, R.V., 1995, Sedimentary organic matter. Organic facies and palynofacies. Chapman and Hall, 615p.

Vail, P.R., Jr. R. M. Mitchum and S. III. Thompson, 1977, Seismic stratigraphy and global changes of sea level, part 3. Relative changes of sea level from coastal onlap: Seismic Stratigraphy — Applications to Hydrocarbon Exploration, AAPG Memoir, v. 26, p. 63–81.

Van Wagoner, J.C., R.M. Mitchum, K.M. Campion, and V.D. Rahmanian, 1990, Siliciclastic sequence stratigraphy in well logs, cores and outcrops: concepts for high resolution correlation of time and facies: AAPG Methods in Exploration Series, v. 7, 53 p.

Woodford Oil Congress 2014 <http://www.woodford-shale-oil-congress.com/> Accessed February 26, 2014.

APPENDIX A: PARASEQUENCES CORRELATION IN THE CHEROKEE PLATFORM

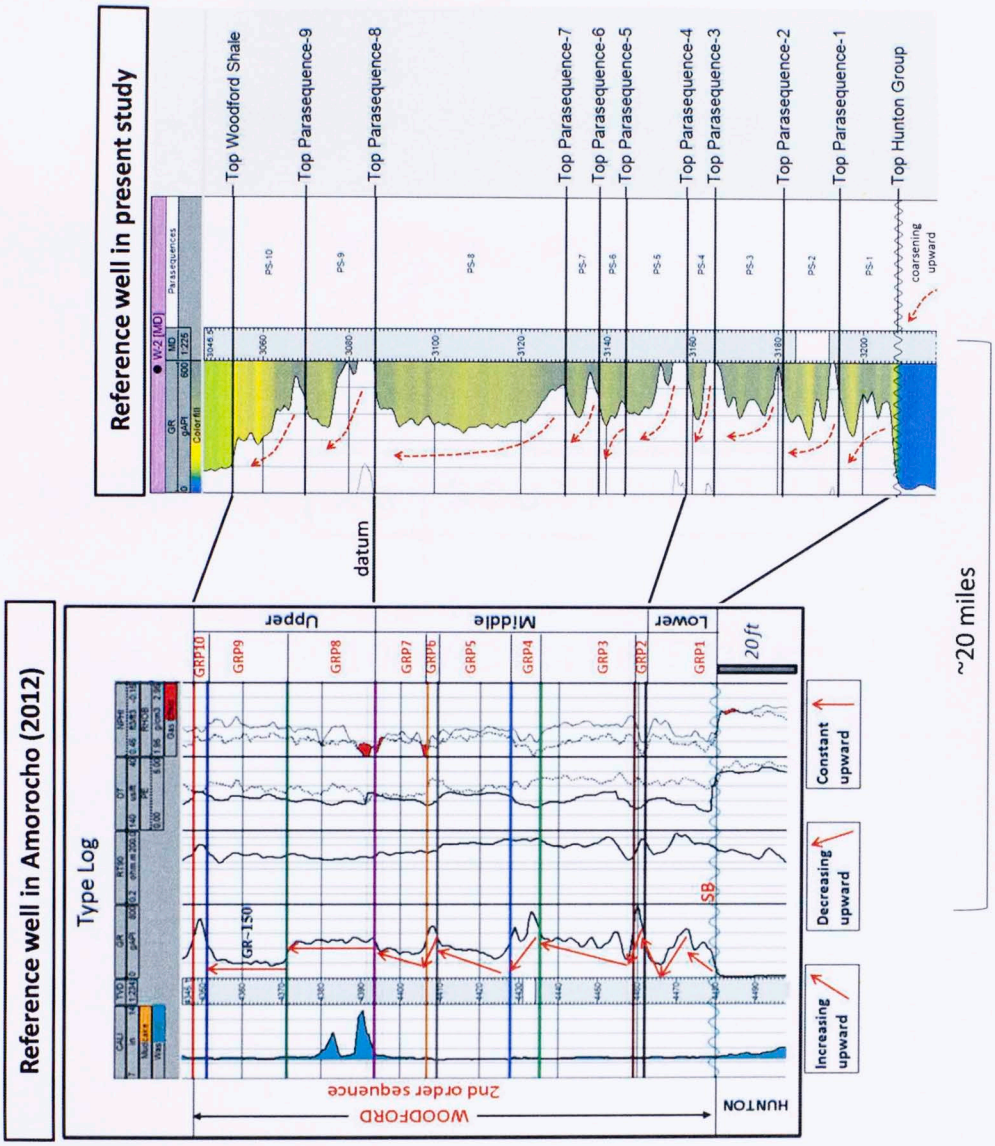

APPENDIX B: TIME-DEPTH CONVERSION FUNCTIONS

1. Woodford Formation time-to-depth conversion function:

$$Y(feet) = 3.72 * X(milliseconds) + 454.48$$

2. Hunton Group time-to-depth conversion function

$$Y(feet) = 4.87 * X(milliseconds) + 1186.7$$

3. Sylvan Shale time-to-depth conversion function

$$Y(feet) = 4.38 * X(milliseconds) + 824$$